[1]

Localisation of TRP Channels in Mammalian Skin

Department of Biology, Lund University

REBEKAH SOPHIA SHERIDAN BECK

Master Thesis in Molecular Biology
45 credits
Supervisor: Prof. Ronald Kröger
Co-supervisor: Prof. Rolf Elofsson
Date: 10/06/15

Abstract

Perception of temperature in mammals is critical for their survival, it enables them to perceive the world around them and act with an appropriate physiological or behavioural response. However, the full understanding of the thermosensory system in mammals has thus far been clouded. TRP channels are thermally sensitive and are known to associate with heat sensitive nerve fibers and keratinocytes in the skin. In my study the focus was understanding their thermotransduction in the rhinarium tissue and whether the sensitivity to radiating heat can be improved by keeping the rhinarium at lower temperatures (as observed in dogs). To solve this I attempted to localise TRPV1-4 and TRPM8, using immunohistochemistry, in the dog and bear rhinarium and compared the expression to other tissue types (belly). My results supported a bolometer like system, consisting of superficial TRP channel skin receptors (TRPV2, TRPV4 and TRPM8) and deep TRP channel skin receptors (all five channels). This would indicate that a colder nose would increase sensitivity to radiating heat whilst protecting the rhinarium from noxious heat.

Contents

Abstract 1
Introduction 4
Mammalian Skin: The Basics 4
Mammalian Skin: Thermosensation and Transduction 4
Mammalian Skin: Transient Receptor Potential Cation Channels 7
Aims and Motivations 7
Materials and Method 8
Preparations for Tissue Sectioning 8
Sample Preparation 8
Slide Preparation 8
Controls 9
Toluidine Blue: Basic skin staining 9
Immunohistochemical Protocols 9
Basic Immunofluorescence Protocol 9
Antigen retrieval 10
Method 1: 2M Hydrogen Chloride (HCL) in PBS 10
Method 2: 0.1% Trypsin in PBS 10
Peroxidase anti-Peroxidase (PAP) with 3 ‘3 Diaminobenzidine tetrahydrochloride hydrate (DAB) 10
Auto-fluorescence and background staining removal techniques 10
Method 1: Acetone treatment with 30mM Sodium Citrate buffer incubation 10
Method 2: Ethanol series 10
Method 3: Photo-bleaching 10
Method 4: Pigmentation removal 10
Microscopy 11
Results 11
Mammalian Skin: Auto-fluorescence Controls 11
Mammalian Skin: Auto-fluorescence Removal 16
Localisation of TRPV1 17
Localisation of TRPV2 18
Localisation of TRPV3 20
Localisation of TRPV4 21
Localisation of TRPM8 23
Mammalian Skin: Localisation of Nerve Network 24

Discussion 28
Mammalian Skin: Auto-fluorescence 29
Mammalian Skin: Feeling the Heat 30
TRPV1's role in thermosensation 30
TRPV2's role in thermosensation 30
TRPV3's role in thermosensation 31
TRPV4's role in thermosensation 32
Mammalian Skin: Feeling the Cold 32
TRPM8's role in thermosensation 32
Mammalian Skin: The Nerve Network 33
Summary: Location of Superficial and Deep TRP Channel Skin Receptors 33
Concluding Remarks 34
Acknowledgments 34
Works Cited 35

Introduction

Mammalian Skin: The Basics

The first line of defence between the outside world and inside an animal is the epidermis, outermost skin layer. It is an effective barrier against physical, chemical and pathogenic assault[3]. However, the skin is not only a barrier but a sensory organ enabling animals to sense the surrounding environment, provoking appropriate responses for animal survival.

There are two main types of skin; thin skin (hairy), which makes up nearly all the skin on the body, and glabrous skin (hairless), is found exclusively in areas like the paw and rhinarium (naked nose tip).

Unspecialised thin mammalian skin is comprised of multiple layers, all with specific functions. The epidermis has a highly active inner basal layer, consisting of a single row of keratinocytes and melanocytes located at the tip of the epidermal pegs (Figure 1)[4]. This layer functions as the site of keratin renewal and pigment production to protect against UV radiation[4]. As the keratinocytes divide they proceed outwards to form the spinous layer, which is several layers thick. Bordering this layer is the granular layer, which consists of only a few layers of keratinocytes and is the location where keratin begins to accumulate. Lastly, the thick outermost cornified layer of the epidermis is where the cells lack a nuclei and function as a barrier to foreign substances.

The outermost layer of the dermis is the stratum papillare which sits below the epidermis. This layer consists of randomly distributed dermal papilla that project into the epidermis, providing structural support. The dermal papilla contain terminal blood vessels and nerves reaching towards the surface of the skin[5]. The inner layer is the reticular layer that consists of mostly collagen and elastin giving the skin flexibility and strength. The reticular layer contains sweat glands, oil glands, blood vessels and hair follicles. The innermost layer which lies below the dermis is the subcutaneous fat layer, the hypodermis, which aids in insulating the body[6].

The rhinarium and paw skin can be defined as specialised glabrous skin due to their differences from the mammalian thin skin. The rhinarium is the wet, hairless area around the nostrils of the nose and is found in most mammals. It has been observed that certain mammals maintain their rhinarium at a cooler temperature than their body for periods of time[7]. Furthermore, the rhinarium's corneal layer forms polygonal plates, which are packed together and divided by grooves into polygonal plaques[8]. Whereas the paws corneal layer forms highly keratinised conical projections that can be seen by the naked eye[8].The corneal layer is far thicker within the glabrous skin than in mammalian thin skin. Additionally the rhinarium and paw skin contain dermal papilla and epidermal pegs which are more uniform in structure and more pronounced than in mammalian thin skin, with the dermal papilla extending towards the surface of the skin, to form patterns seen by the naked eye[9]. The distinct differences between the skin types used in this project can be seen in figure 1.

Mammalian Skin: Thermosensation and Transduction

Thermosensation is crucial for mammals to correctly judge their environment. This valuable information provokes involuntary (physiological) or voluntary (behavioural) actions over a wide range of temperatures[10, 11]. It is crucial for animal survival allowing escape response against noxious heat and cold, or attraction responses towards preferable temperatures[10]. Interestingly, recent thermal studies have shown that glabrous skin in dogs can be as cold at 0.5°C without the animal showing signs of discomfort[12]. Therefore, mammalian thermosensitivity and limits for noxious temperatures cannot be generalised.

The sensory cells which respond to temperature as well as pain, pressure and touch are distributed throughout the epidermal and dermal layers of the skin. The transduction of these stimuli primarily relies on unique somatosensory neurons which reside in the trigeminal and dorsal root ganglia and have axonal processes that extend into the outer layers of skin[10]. The sensory neurons use dendrites to gather information relating to their environment, the detected information is then transduced via axons to the brain to be processed. The epidermis and dermis are penetrated throughout by free nerve endings of Aδ and C fibres. Aδ-fibres typically exhibit medium-sized cell bodies, thinly myelinated axons and intermediate conduction velocities[11]. C-fibres on the other hand exhibit small cell bodies, no myelin sheath and slow conduction velocities[11]. Both types of fibres aid in thermotransduction and are nociceptive fibers responding to potentially damaging stimuli[11]. Specific

thermosensitive channels are believed to be associated with these free nerve endings**,** working in concert to orchestrate an appropriate response over a wide range of temperatures[10]. Once thermally stimulated the thermosensitive channels cause depolarisation of the free sensory nerve endings, generating action potentials, which travel from the periphery to the central nervous system (CNS) eliciting a response[11].

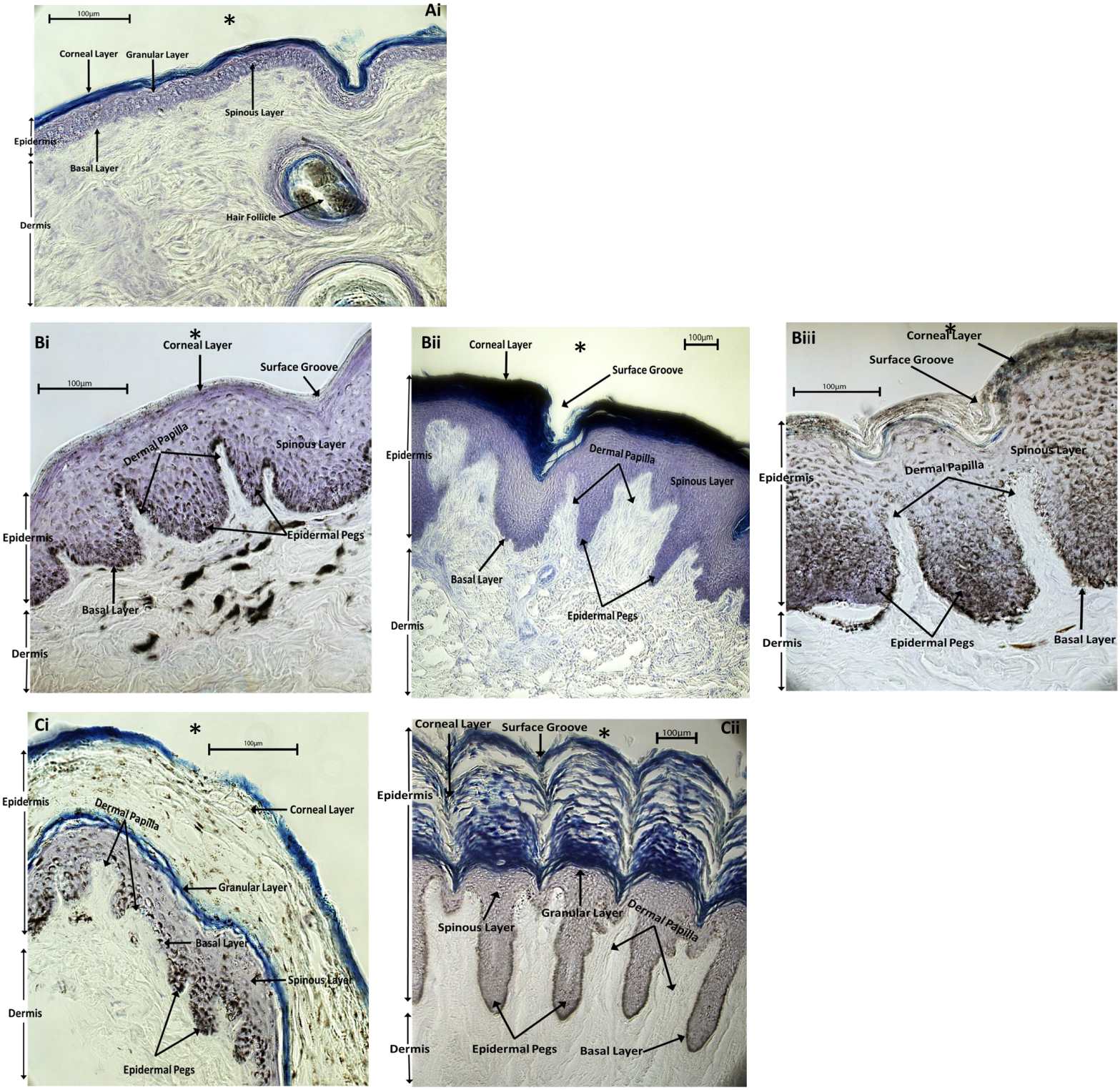

Figure 1: Skin reference images: *Blue* ***Ai****: Dog belly skin (other species not shown as skin structure was almost identical).* ***Bi****: Dog rhinarium skin.* ***Bii****: Bear rhinarium skin.* ***Biii****: Lemur rhinarium skin.* ***Ci****: Dog paw skin.* ***Cii****: Lemur paw skin. Tissue sections are 12 µm thick and stained with Toludin.* Asterisks indicates orientation of tissue section, indicating skin surface. *Scale: 100 µm.*

Mammalian Skin: Transient Receptor Potential Cation Channels

The thermosensitive channels believed to be involved in thermosensation is the Transient Receptor Potential (TRP) cation channels. However, the function of each TRP channel and their role in thermosensation is still not fully understood, calling for further research to be carried out. Besides this, they are a diverse polymodal family of 28 cation channels which also have roles in chemosensation, mechanoreception, osmoreception, magnesium transport and iron transport[13]. Nevertheless, structurally all members of the TRP channel superfamily have 6 transmembrane domains, of which 4 subunits form the non-selective cation channel[11]. Thermosensitive TRP channels have evolved thermal response profiles which collectively cover the entire range of temperatures that mammals can discriminate, ranging from 8-52°C[11]. Herein, only the TRP channels V1-4 and M8, that can be found in the mammalian skin, will be discussed as they were the focus of this study. At present there is strong evidence that illustrates TRPV1-4 are involved in heat sense and TRPM8 is involved in cold sense, however there is still some areas lacking confirmed results.

TRPV1 (Capsaicin receptor or Vanilloid receptor 1) and TRPV2 are known to be stimulated by noxious heat, with a stimulus range above 43°C and 52°C respectively[14]. The channels themselves have non-selective cation permeability, like most TRP channels, however they do have a preference for Ca^{2+} ions[14]. A quality of TRPV1 unlike the other TRP channels is its sensitivity to capsaicin, a chemical compound active in chili peppers[14]. Both, TRPV1 and TRPV2 have been found to be expressed in multiple locations throughout the skin[15]. However TRPV2 has only been proven to be stimulated by noxious heat in vitro[15].

TRPV3 and TRPV4 are molecular sensors involved in the detection of non-noxious heat, having a stimulus range of 34-38°C and 28-42°C respectively[14, 15]. Interestingly, there seems to be conflicting ideas on the level of expression of both channels in the sensory neurons, some determining that there is low to non-existent expression and others illustrating normal levels [11, 15-17]. However, expression within the epidermal and hair-follicle keratinocytes has been confirmed[11].

While TRPV1-4 are believed to play significant roles in heat detection, TRPM8 is distinct from the rest as it is responsive to cool or cold temperatures. Its temperature stimulus range is 15-28°C therefore, its temperature dependence extends from cool to noxious cold[14, 15]. This channel is also stimulated by menthol, a cooling compound, which increases the activation temperature threshold of TRPM8. Like the other TRP channel TRPM8's expression has been located to C and Aδ fibres which respond to changes in temperature[11, 15].

Aims and Motivations

The motivations for this study was mainly due to the specific observations seen within dogs. The first observation was they frequently have their rhinarium sitting at cooler temperatures than their own body. The second observation was of several dogs that had extremely low rhinarium temperatures without any indication of discomfort.

These observations and the belief that the rhinarium is an important sensory organ for foraging and hunting, often being a point of contact with the ground, makes it interesting to investigate if maintaining a cool rhinarium is linked to sensing radiating heat. Furthermore, it would be of interest to explore how different mammals protect their naked rhinarium skin in varying climates and if this is different to other tissue types. Whilst investigating this I was hoping to reduce the level of confusion in TRP-channel research by using more variable tissues and several mammalian species. As at present there is a strong bias towards the use of the paw and tail of laboratory rodents in TRP channel research which are maintained within ambient temperatures.

The first focus was to use immunohistochemistry to discover the locations of TRPV1-4 and TRPM8 channels in dog rhinarium tissue, to determine if their locations would enable sensitivity to radiating heat. This was followed by comparing TRP channel expression in rhinarium skin to other types of skin such as the belly and paw, the belly being the least environmentally exposed and the paw being exposed to harsh mechanical and thermal stimuli. This would allow determination of any differences in TRP channel expression in the mentioned tissue types and whether it is dependent on the degree of environmental exposure. Leading to the final focus, the comparison of mammals from

different climates to determine if certain channels are over or under represented due to the selective pressure of the climate. This would also hopefully reduce the current model organism bias in TRP channel research.

Materials and Method

Table 1 – General information on tissues used for Immunohistochemical experiments: *The Köppen Climate Classification indicated the type of climate the animal inhabits.*

Mammal	Breed or Species	Köppen Climate Classification	Tissues used (Yes/No)			Cause of death	Time between death and fixation	Source of tissue/ Storage notes
			Nose	Paw	Belly			
Dog A	Maltese	N/A	Y	N	Y	Age related	17 hours	Argentina vet clinic/ > 1 month in Phosphate buffer at 4°C
Dog B	Golden Retriever	N/A	Y	N	Y	Generalized bleeding	7 hours	Argentina vet clinic/ Frozen at -80°C
Dog E	Mixed breed	N/A	Y	N	N	Lymphoma	~1 hour	Argentina vet clinic/ Frozen at -80°C
Dog F	Maltese	N/A	Y	N	Y	Haemorrhage	2.5 hours	Argentina vet clinic/ Frozen at -80°C
Primate	Ring-tailed Lemur (*L. catta*)	wet subtropical	Y	Y	Y	Euthanasia due to injuries	~1 hour	> 1 month in Phosphate buffer at 4°C
Bear	Brown bear *(U. arctos)*	boreal climates	Y	N	Y	Euthanasia	~1 hour	skåne djurparken / < 1 day in Phosphate buffer at 4°C

Preparations for Tissue Sectioning

Sample Preparation

To fixate the tissue sample it was incubated at room temperature overnight in 4% paraformaldehyde in 0.1 M Sörensensphosphate buffer. 0.1 M Sörensensphosphate buffer was prepared by adding 28 ml of Stock A and 72 ml of Stock B to 100 ml of distilled H_2O, see Table 2 for stock recipes, adjust to pH 7.2. The tissue was then washed with 0.1 M Sörensensphosphate buffer, 3 times for 10 minutes at room temperature. To prepare the tissue for sectioning it was infiltrated in 25% sucrose with phosphate buffer saline (PBS) overnight at 4°C. PBS was prepared via addition of 80 ml Stock 1 and 20 ml Stock 2 to 8.5 g NaCl in 900 ml of distilled water, see Table 2 for stock recipes. Prior to cryo-sectioning the tissue was removed from the sucrose and positioned in desired orientation. Embedding medium (Richard-Allan Scientific, NEG 50™, Thermo-Scientific) was poured on the sample, and frozen at -50°C, while continuing to add more embedding medium until the tissue sample is entirely covered. A flat edge was created and the sample was attached to a metal holder via freezing and secured by adding more embedding medium. The holder was then mounted in the holder in the cryostat, keeping the sample at -20°C and was then sectioned (12 µm).

Slide Preparation

Two g of gelatin was mixed with 200 ml of dH_2O and dissolved on a hot plate (60°C). In a separate flask 0.2 g chrome alum ($KCr(SO_4)_2$ x $12H_2O$) was mixed with 200 ml of dH_2O. These two mixtures were mixed together and filtered. Glass slides were cleaned with 96% ethanol and dipped in the Chromalumgelatin solution. The slides were left to dry over night at 60°C.

Table 2 – Stock solution recipes for buffers used in Immunohistochemical protocols.

Stock Name	Compound	Weight in 100 ml of distilled water	Buffer used in
Stock A	NaH_2PO_4 x H_2O	2.76 g	Sörensensphosphate buffer
Stock B	Na_2HPO_4	2.84 g	Sörensensphosphate buffer
Stock 1	Na_2HPO_4	1.4 g	Phosphate buffer saline
Stock 2	NaH_2PO_4 x H_2O	1.6 g	phosphate buffer saline

Controls

Tissue sections were washed in PBS with 0.25 % Triton (PBS/TX) twice for 10 minutes at room temperature, then washed in PBS three times for 10 minutes at room temperature and mounted in a 1:9 glycerin/PBS solution. The edges were sealed with nail polish.

Toluidine Blue: Basic skin staining

The tissue slides were rinsed in distilled H_2O then stained for 1 minute (1.5 minutes for belly tissue) in Toluidine Blue Solution. The residual stain was removed via a quick rinse in 70 % ethanol, 1 minute in 96 % ethanol, 5 minutes in 100 % ethanol twice and then 5 minutes in xylene twice. The tissue sections were mounted and coverslipped using entellan.

Immunohistochemical Protocols

Basic Immunofluorescence Protocol

A fat barrier was created around the tissue sections. The sections were then washed for 10 minutes in PBS/ TX twice at room temperature. Tissue sections were incubated in 10% of the appropriate normal serum in dilution buffer (PBS with 0.25% TX and 1% Bovine Serum Albumin (BSA)) for 30 minutes. Tissue sections were incubated overnight in a humid chamber with the appropriate concentration of primary antibody in dilution buffer (Table 3). Sections were then washed for 10 minutes twice in PBS/TX buffer, then incubated with the appropriate concentration of secondary antibody for one hour in the dark at room temperature (Table 3). The sections were then washed three times for 10 minutes in PBS/TX and twice in PBS for 10 minutes. The slides were mounted in a 1:9 glycerin/PBS solution and the edges sealed with nail polish.

The basic immunofluorescence protocol was adapted by inclusion or exclusion of BSA. However the results from the antigen retrieval are not shown due to being inconclusive.

Table 3 – Antibodies used for immunohistochemistry

	Name	Host [Epitope]	Concentration	Company
Primary's				
	Trpv1 polyclonal antibody	Rabbit	1:10	Abnova
	Trpv2 polyclonal antibody	Rabbit	1:100	Abnova
	Trpv3 polyclonal antibody	Rabbit	1:500	Abnova
	Trpv4 polyclonal antibody	Rabbit	1:200 / 1:500	Abnova
	Anti-TRPM8 polyclonal antibody	Goat	1:300	Abcam
	Neurofilament 200, polyclonal	Rabbit	1:800	Sigma
Secondary's	Chicken anti-Rabbit IgG (H+L)Secondary Antibody, Alexa Fluor® 488 conjugate	Chicken [Rabbit]	1:200	Life Technologies
	Donkey anti-Goat IgG (H+L) Secondary Antibody, Alexa Fluor® 546 conjugate	Donkey [Goat]	1:600	Life Technologies

Antigen retrieval

The basic immunofluorescence protocol was followed and the antigen retrieval methods were carried out after the first wash of the tissue sections in PBS/TX.

Method 1: 2M Hydrogen Chloride (HCL) in PBS

Stock 1 (40 ml) was mixed with Stock 2 (10 ml), Table 2. Sodium Chloride (0.29 g) was added to the PBS buffer along with 12M HCL (16 ml) and distilled water (34 ml). The tissue sections were incubated in 2M HCL in PBS for 15 minutes at room temperature.

Method 2: 0.1% Trypsin in PBS

Calcium chloride dihydrate (0.13 g) was dissolved in PBS (100ml) and the pH was adjusted to pH 7.8 using sodium hydroxide. Trypsin (0.1 g) was dissolved in the calcium chloride solution. The tissue sections were incubated in this solution at 37°C for 25 minutes.

Peroxidase anti-Peroxidase (PAP) with 3 '3 Diaminobenzidine tetrahydrochloride hydrate (DAB)

A fat barrier was created surrounding the tissue sections. The tissue sections were washed in PBS/TX twice for 10 minutes at room temperature. The appropriate primary antibody was diluted in dilution buffer (Table 3). The tissue sections were incubated overnight with the appropriate primary antibody in a humid chamber at room temperature. The tissue sections were washed in PBS/TX twice for 10 minutes. The secondary antibody was diluted to the appropriate concentration in dilution buffer (Table 3). The sections were incubated with the appropriate secondary antibody for 1 hour in a humid chamber (in the dark). They were then washed in PBS/TX after incubation, twice for 10 minutes. The PAP complex was diluted in dilution buffer (1:50) and incubated with the tissue sections for 45 minutes in a humid chamber. The sections were washed in PBS/TX for 10 minutes then in 0.05 M Tris-HCL (pH 7.6) for 10 minutes. The DAB solution was then prepared in a fume hood. DAB preparation involved adding 1 DAB ampoule to 50 ml Tris-HCL buffer and 250 µl of 3% H_2O_2. The solution was mixed in the dark and used immediately. The tissue sections were incubated with the DAB/Tris/HCL solution for 10 minutes (in the dark) in a fume hood. The slides were washed under running tap water for 10 minutes. Once rinsed the tissue was dehydrated using an ethanol series and two washes in xylene. The tissue sections were then mounted in xylene based mounting media.

Auto-fluorescence and background staining removal techniques

Method 1: Acetone treatment with 30mM Sodium Citrate buffer incubation

The tissue sections were washed in PBS/TX twice for 10 minutes then immersed in chilled acetone for 20 minutes. The tissue sections were then washed twice in PBS for 10 minutes followed by incubation in 30 mM Sodium citrate buffer (0.44 g sodium citrate trisodium salt dehydrate dissolved in 50 ml deionised water) (pH 8.8) for 30 minutes at 60°C. The tissue sections were then washed twice in PBS for 10 minutes. The basic immunofluorescence protocol was then carried out.

Method 2: Ethanol series

The tissue sections were washed in PBS/TX twice for 10 minutes then put through a series of PBS and ethanol (76 % then 96%, 3 minutes each). The tissue sections were then washed twice in PBS for 10 minutes. The basic immunofluorescence protocol was then carried out.

Method 3: Photo-bleaching

Tissue sections pre-treated using Method 1 or Method 2 of the auto-fluorescence removal method were subjected to intense light overnight. The tissue sections were then viewed on the microscope.

Method 4: Pigmentation removal

The basic PAP with DAB protocol was carried out until the first tissue section wash in PBS/TX. The tissue sections were then incubated in 10% Hydrogen Peroxide (H_2O_2) in PBS for 10 minutes at room temperature. The basic PAP with DAB protocol was then followed.

Microscopy

The tissue sections were visualised using a Zeiss - DSFi1c microscope with an attached Nikon - D.4.20.01 65 – bit camera. A Fitc filter cube was used to view tissue incubated with Alexa Fluor® 488 secondary antibody and a Tritc filter cube was used to view tissue incubated with Alexa Fluor® 546.

Results

Due to severe auto-fluorescence within the skin samples initially used the direction of this project moved towards solving this problem primarily in the dog rhinarium tissue and optimising the handling protocols for these specific tissues. However, some tissues (paw and lemur) had to be abandoned from the study. Furthermore, the results described here were observed in multiple sections, illustrating the consistency of TRP channel signal. Any results that appeared in a single section will be discussed later, providing reasons why this may have occurred. Lastly, All the TRP channel localisation results in mammalian skin are summarised in Table 4.

Mammalian Skin: Auto-fluorescence Controls

Auto-fluorescence control images, were no primary or secondary antibody was used illustrated that the dog rhinarium, belly and paw tissue had varying degrees of auto-fluorescence (Figure 2-4). Dog A's rhinarium tissue had heavy auto-fluorescence (Figure 2: Image A-B), however, the previously frozen dog B's rhinarium tissue had far less auto-fluorescence (Figure 2: Image C). Whereas the previously frozen dog F and dog E's rhinarium tissue, had little to no auto-fluorescence present (Figure 2: Image D-E). The level of auto-fluorescence somewhat decreases as the time between death of the animal and fixation of the tissue decrease (Table 1 and Figure 2). The dog A's belly showed high auto-fluorescence in both filters (Figure 3: Image A-B). Whereas, the previously frozen dog F's belly tissue shows low levels of auto-fluorescence in both filter (Figure 3: Image C-D). The dog A's paw tissue illustrates high levels auto-fluorescence in both filters (Figure 4: Image A-B). The auto-fluorescence can be seen in the images as irregular green or red structures within the tissue.

Auto-fluorescence control images for the lemur rhinarium, belly and paw tissue all illustrated auto-fluorescence in both filters (Figure 5-7). The auto-fluorescence can be seen in the images as irregular green or red structures within the tissue.

Auto-fluorescence control images for the bear rhinarium and belly illustrated no auto-fluorescence (Figures 8 and 9). All tissue from the bear showed no signs of auto-fluorescence in either filters as all images are black.

Auto-fluorescence control images, using just the secondary antibody and no primary antibody in all three species of animal and tissue type produced the same images, however, they are not shown.

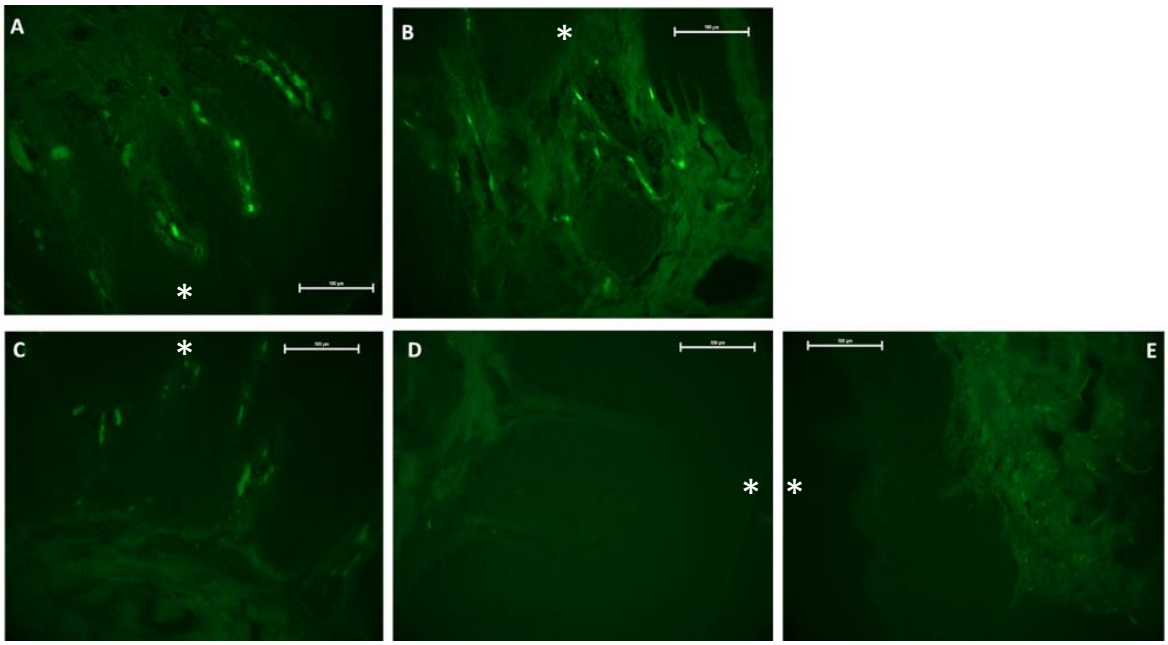

Figure 2: Dog rhinarium auto-fluorescence control images (no antibodies used); A/B: dog A rhinarium tissue (stored at 4°C). C: dog B rhinarium tissue (stored at -80°C). D: dog F rhinarium tissue (stored at -80°C). E: dog E rhinarium tissue (stored at -80°C). Time between death of animal and fixation of tissue increases from A to E (Table 1). Auto-fluorescence is indicated by unstructured green blobs. Asterisks indicates orientation of tissue section, indicating skin surface. Scale: 100 µm

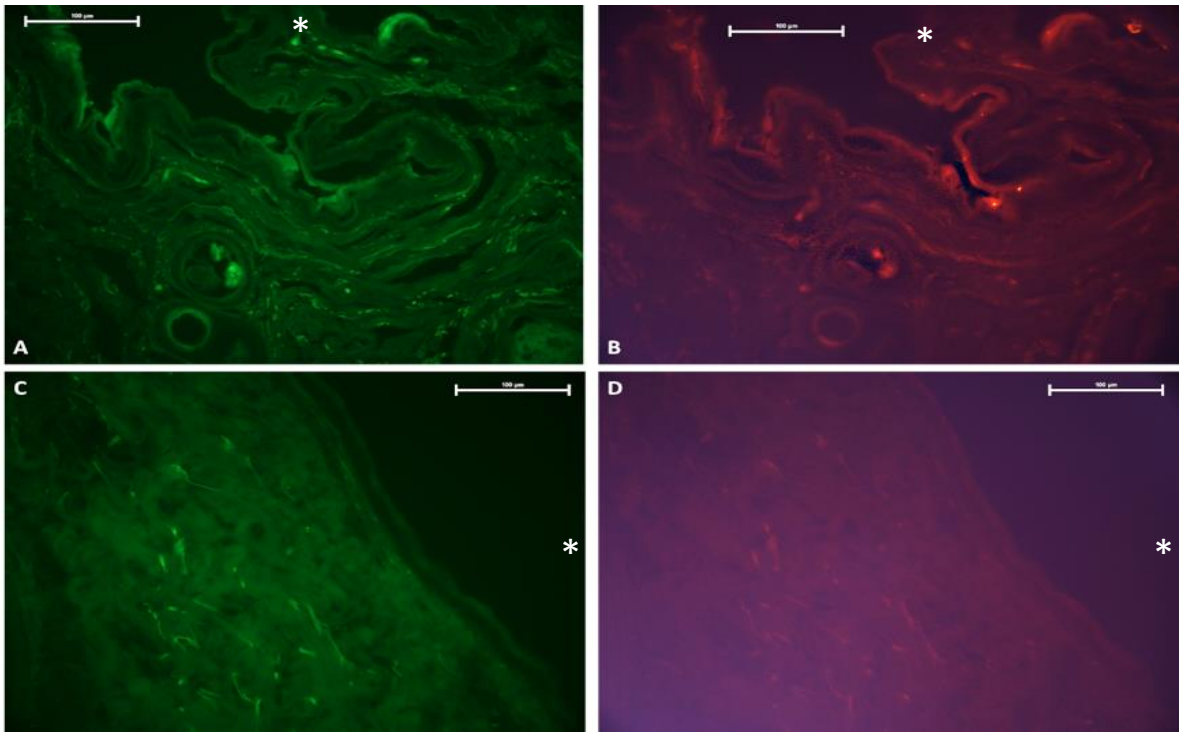

Figure 3: Dog belly auto- fluorescence control images (no antibodies used); A/C: Dog A and F belly tissue respectively using Fitc filter cube. B/D: Same tissue location as image A/C however using the Tritc filter cube. Auto-fluorescence is indicated by unstructured green and red blobs. All images show high levels of auto-fluorescence. Asterisks indicates orientation of tissue section, indicating skin surface. Scale: 100 µm

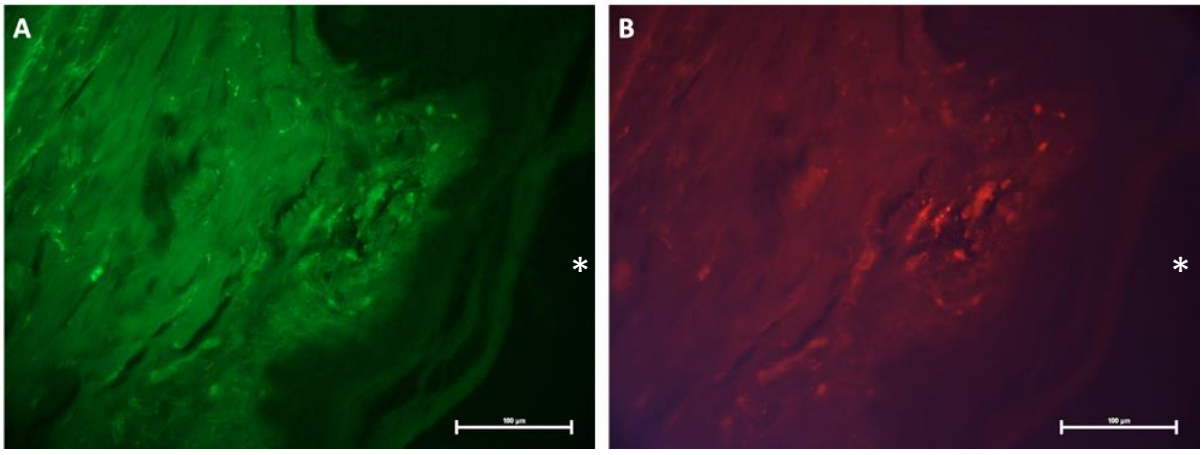

Figure 4: Dog A's Paw auto-fluorescence control images (no antibodies used); A/B: dog A paw tissue using Fitc and Tritc filter cube respectively, images are taken at the same location. Auto-fluorescence is indicated by unstructured green and red blobs within the dermis. Both images show high levels of auto-fluorescence. Asterisks indicates orientation of tissue section, indicating skin surface. Scale: 100 µm

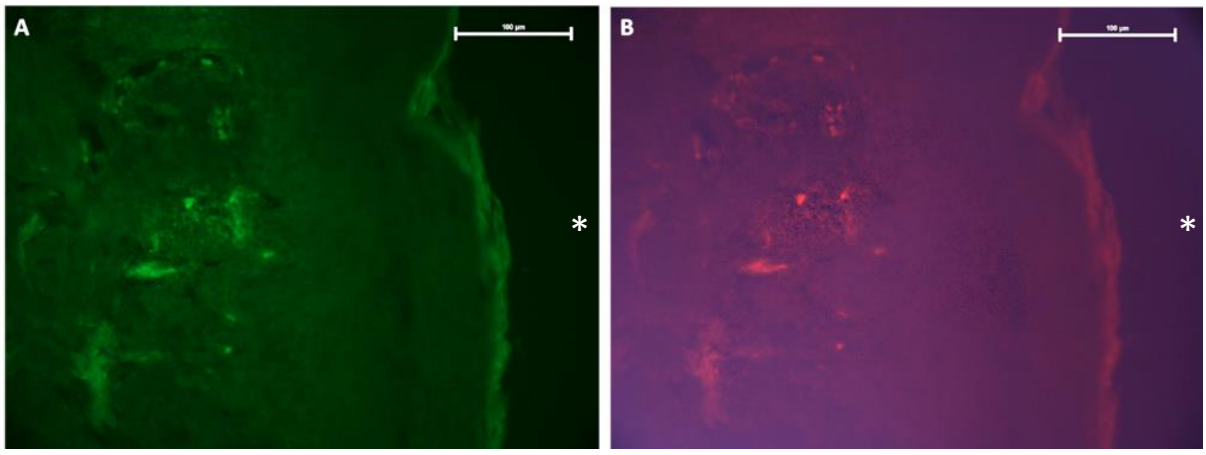

Figure 5: Lemur rhinarium auto-fluorescence control images (no antibodies)*;* A/B: lemur rhinarium tissue using Fitc and Tritc filter cubes respectively, images are taken at the same location. Auto-fluorescence is indicated by unstructured green and red blobs within the dermis. Both images show high levels of auto-fluorescence. Asterisks indicates orientation of tissue section, indicating skin surface Scale: 100 µm

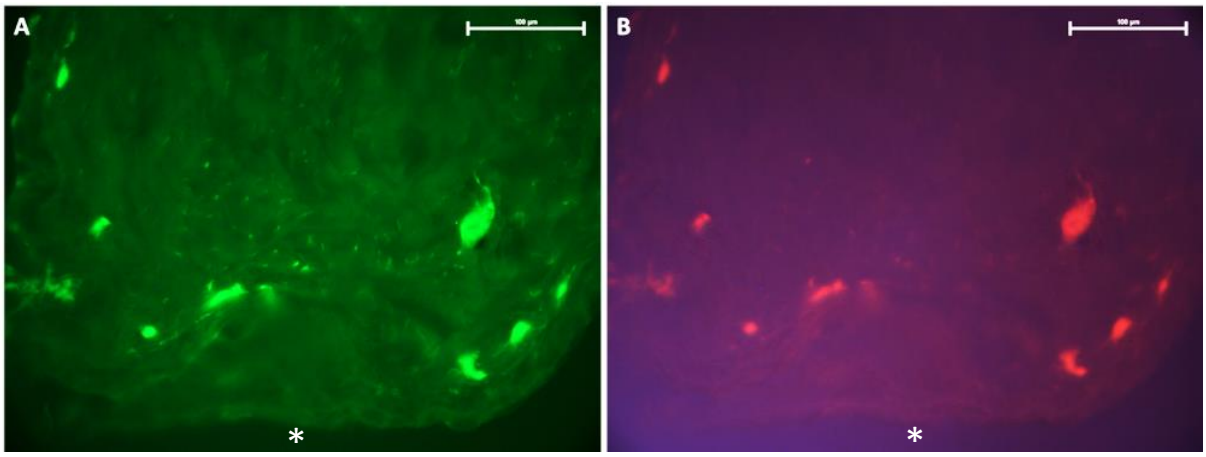

Figure 6: Lemur belly auto-fluorescence control images (no antibodies used); A/B: lemur belly tissue using Fitc and Tritc filter cubes respectively, images are taken at the same location. Auto-fluorescence is indicated by unstructured green and red blobs within the dermis. Both images show high levels of auto-fluorescence. Asterisks indicates orientation of tissue section, indicating skin surface. Scale: 100 µm

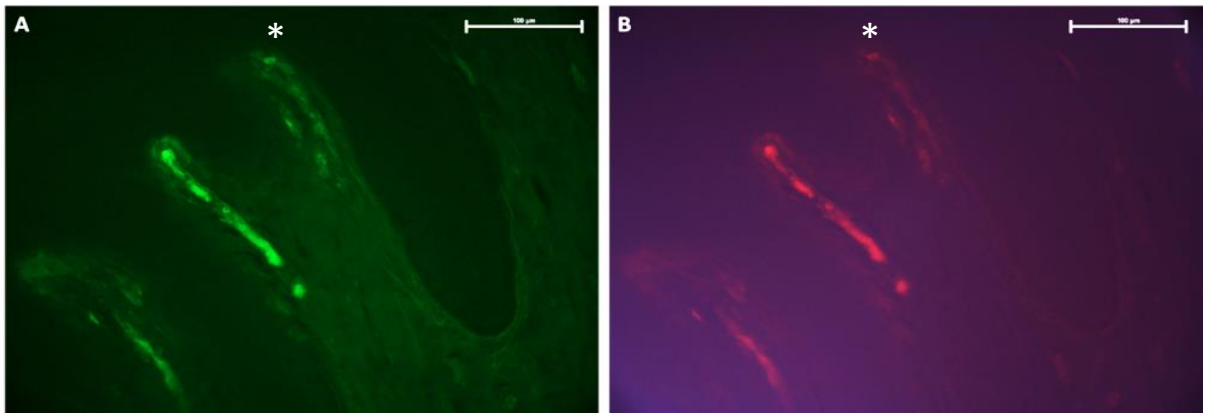

Figure 7: Lemur paw auto-fluorescence control images (no antibodies used); A/B: Lemur paw tissue using Fitc and Tritc filter cubes respectively, images are taken at the same location. Auto-fluorescence is indicated by unstructured green and red blobs within the dermal papilla. Both images show high levels of auto-fluorescence. Asterisks indicates orientation of tissue section, indicating skin surface Scale: 100 µm.

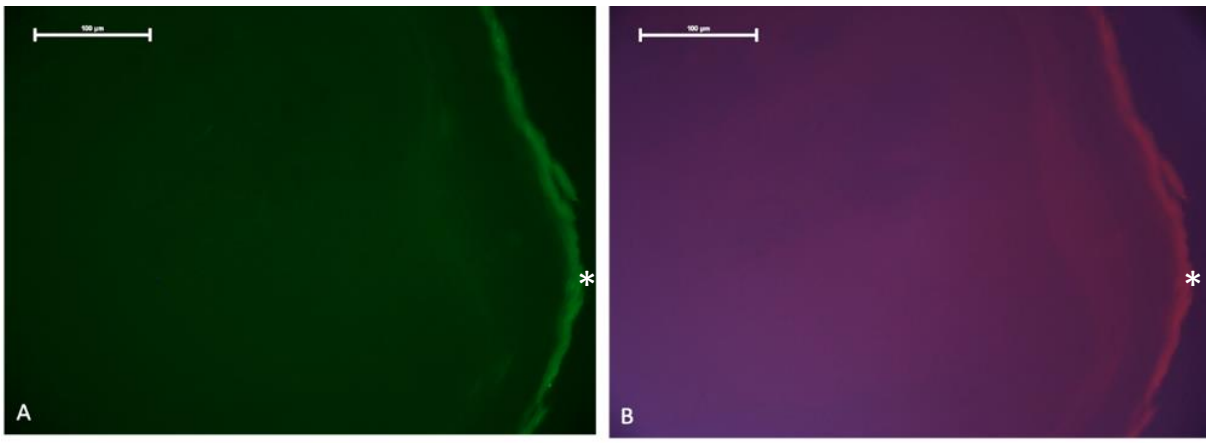

Figure 8: Bear rhinarium auto-fluorescence control images (no antibodies used): A/B: bear rhinarium tissue using Fitc and Tritc filter cubes respectively, images are taken at the same location. There is no auto-fluorescence indicated in either image, no unstructured green or red blobs within the tissue. Asterisks indicates orientation of tissue section, indicating skin surface. Scale: 100 µm.

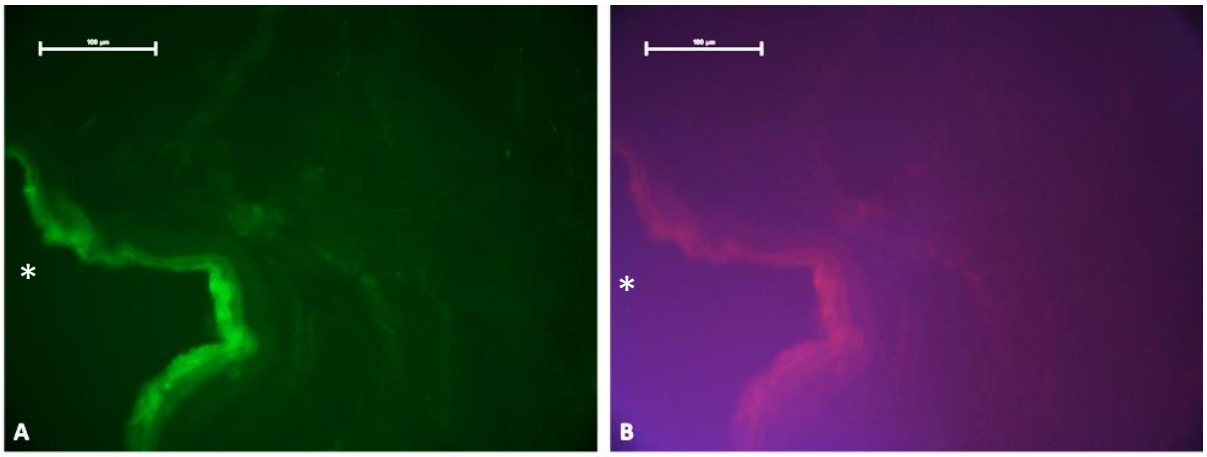

Figure 9: Bear belly auto-fluorescence control images (no antibodies used); A/B: bear belly tissue using Fitc and Tritc filter cubes respectively, images are taken at the same location. There is no auto-fluorescence indicated in either image, no unstructured green or red blobs within the tissue. Asterisks indicates orientation of tissue section, indicating skin surface. Scale: 100 µm.

Mammalian Skin: Auto-fluorescence Removal

All attempts to remove the auto-fluorescence within the dog rhinarium tissue were unsuccessful (Figures 10-13). Dog A's rhinarium tissue still illustrated auto-fluorescence, prominent green structures within the dermal papilla, after removal of BSA from the protocol (Figure 10: Image A-B). Dog A's rhinarium tissue still illustrated auto-fluorescence, prominent green structures, after both ethanol and acetone treatment before mounting (Figure 11: Images A-B). Dog A's rhinarium tissue which underwent an ethanol series or acetone treatment before photo bleaching still illustrated auto-fluorescence, the green structures within the dermal papilla (Figure 12: Image A-B). Lastly, Dog A's rhinarium tissue underwent pigmentation removal, however the tissue was still heavily pigmented after treatment, illustrated by the black/brown structures (Figure 13: Image A-B).

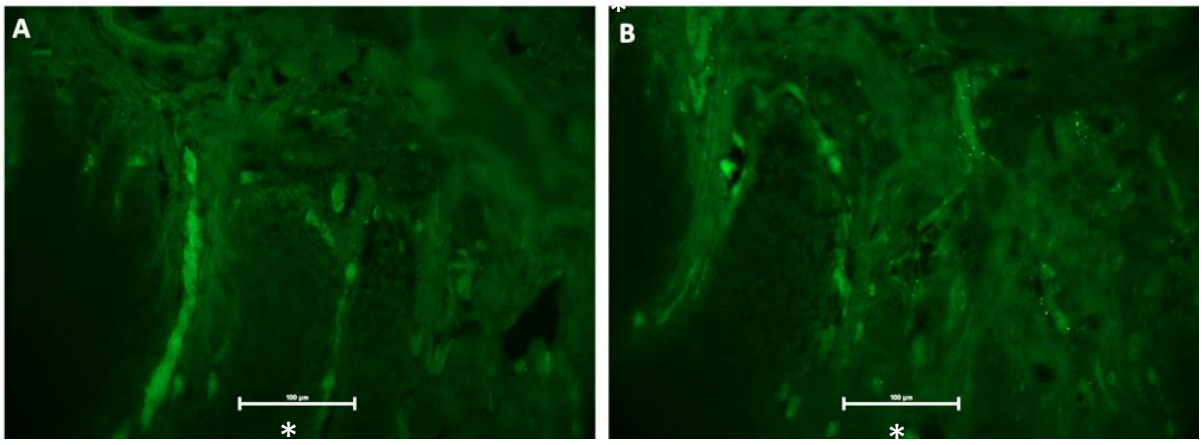

Figure 10: Auto-fluorescence removal: Effect of removing Bovine Albumin Serum; A: dog A rhinarium tissue without the use of BSA in the protocol. B: dog A rhinarium tissue with the use of BSA in the protocol. Auto-fluorescence is still present with or without BSA, indicated by the unstructured green blobs within the dermal papilla and dermis. Asterisks indicates orientation of tissue section, indicating skin surface. Scale: 100 µm

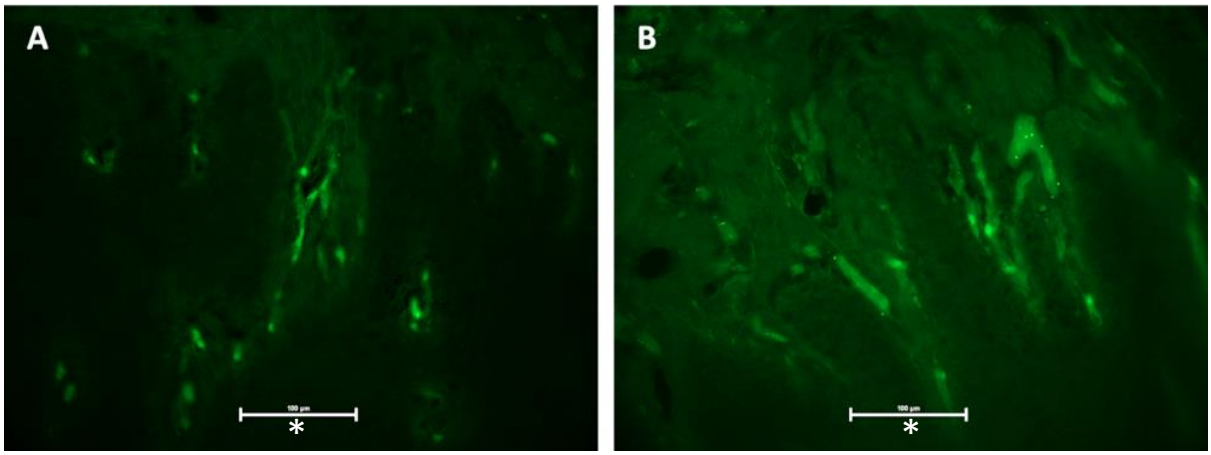

Figure 11: Auto-fluorescence removal: Ethanol Series and Acetone treatment (with Citrate buffer); A: Ethanol series treated dog A rhinarium tissue. B: Acetone treated dog A rhinarium tissue. Auto-fluorescence is still present after both treatments, indicated by unstructured green blobs within the dermis and dermal papilla. Asterisks indicates orientation of tissue section, indicating skin surface. Scale: 100 µm.

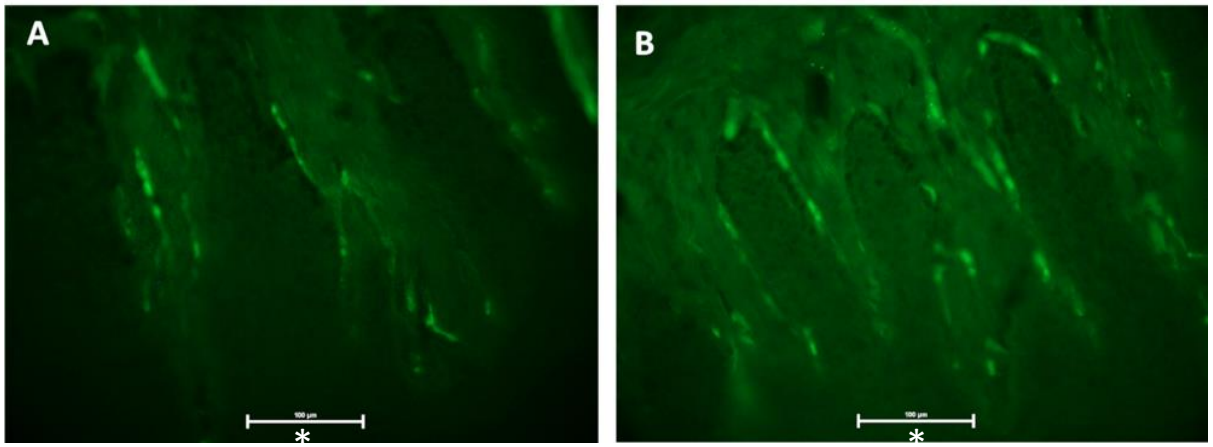

Figure 12: Auto-fluorescence removal: Ethanol Series and Acetone treatment with photo bleaching; A**:** Ethanol series treated dog A rhinarium tissue with photo bleaching. B: Acetone treated dog A rhinarium tissue with photo bleaching. After both treatments and photobleaching auto-fluorescence is still present, indicated by the unstructured green blobs within the dermis and dermal papilla. Asterisks indicates orientation of tissue section, indicating skin surface. Scale: 100 µm

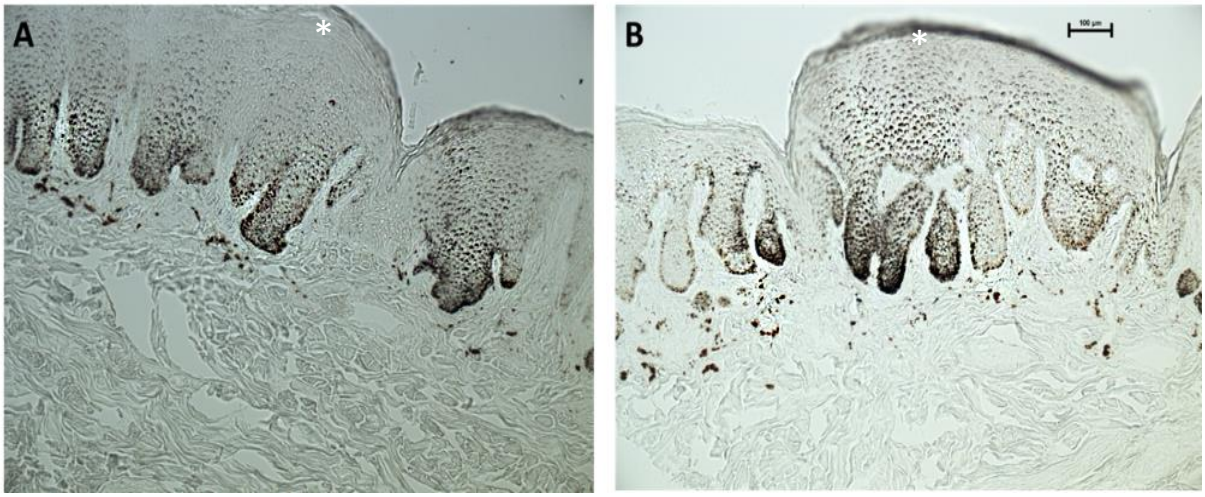

Figure 13: Pigment removal treatment; A: dog A rhinarium tissue without pigment removal treatment. B: dog A rhinarium tissue after pigment removal treatment. Pigment still remains after treatment indicated by the dark pigmented structure. Asterisks indicates orientation of tissue section, indicating skin surface. Scale: 100 µm.

Localisation of TRPV1

The localisation of TRPV1 in specific tissues was observed in various mammalian tissues (Figure 14). TRPV1 signal is present at the bottom of the dermal papilla of dog F's rhinarium, within cells that are not prone to auto-fluorescence (Figure 14: Image A and B). Whereas, the TRPV1 signal is present in the bear rhinarium tissue at the tips of the epidermal pegs (Figure 14: Image D). On the other hand, there is a more diffuse TRPV1 signal throughout the bear belly tissue, in both the epidermis, dermis and hair follicles (Figure 14: Image C).

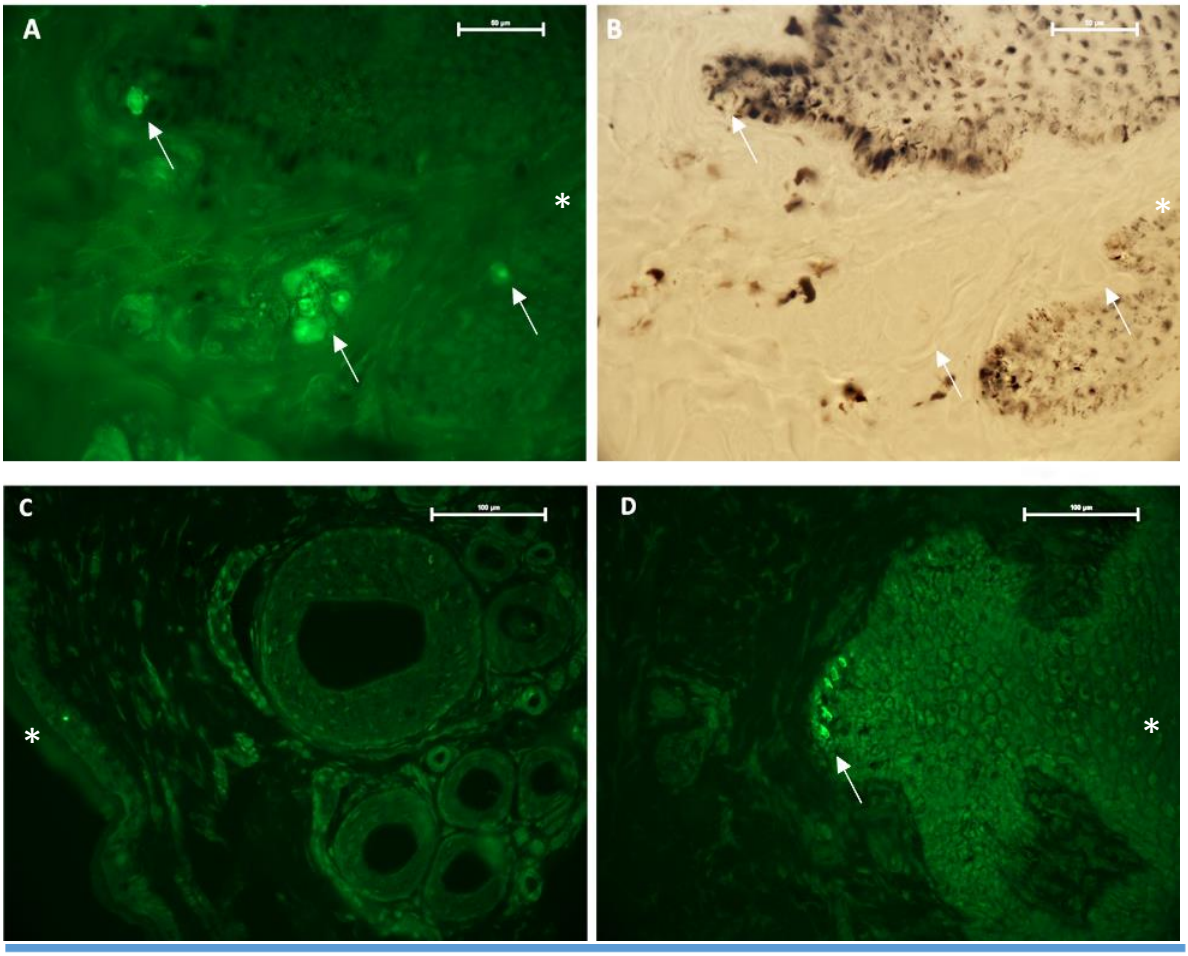

Figure 14: Immunohistochemical localisation of TRPV1 in mammalian skin. A: dog F rhinarium tissue illustrating TRPV1 signal at the bottom of the dermal papilla and epidermal pegs. B: Histological reference image to image A, indicating structural location of TRPV1 signal within the rhinarium tissue. C**:** bear belly tissue, depicting diffuse TRPV1 signal. D: bear rhinarium tissue illustrating TRPV1 signal at the tip of the epidermal pegs. White arrows indicate location of TRPV1 signal. Asterisks indicates orientation of tissue section, indicating skin surface. Scale: 100 µm.

Localisation of TRPV2

The localisation of TRPV2 in specific tissue was observed in various mammalian tissue (Figure 15). TRPV2 signal was present in both the dog and bear rhinarium tissue within a dermal papilla, in a location that seems to not be associated with auto-fluorescence (Figure 15: Image A, B and C). The bear rhinarium also has TRPV2 signal present in the dermis more specifically near the epidermal-dermal border (Figure 15: Image D). Lastly, TRPV2 signal is observed within the hair follicles of the bear belly but not the dog belly (Figure 15: Image E and F).

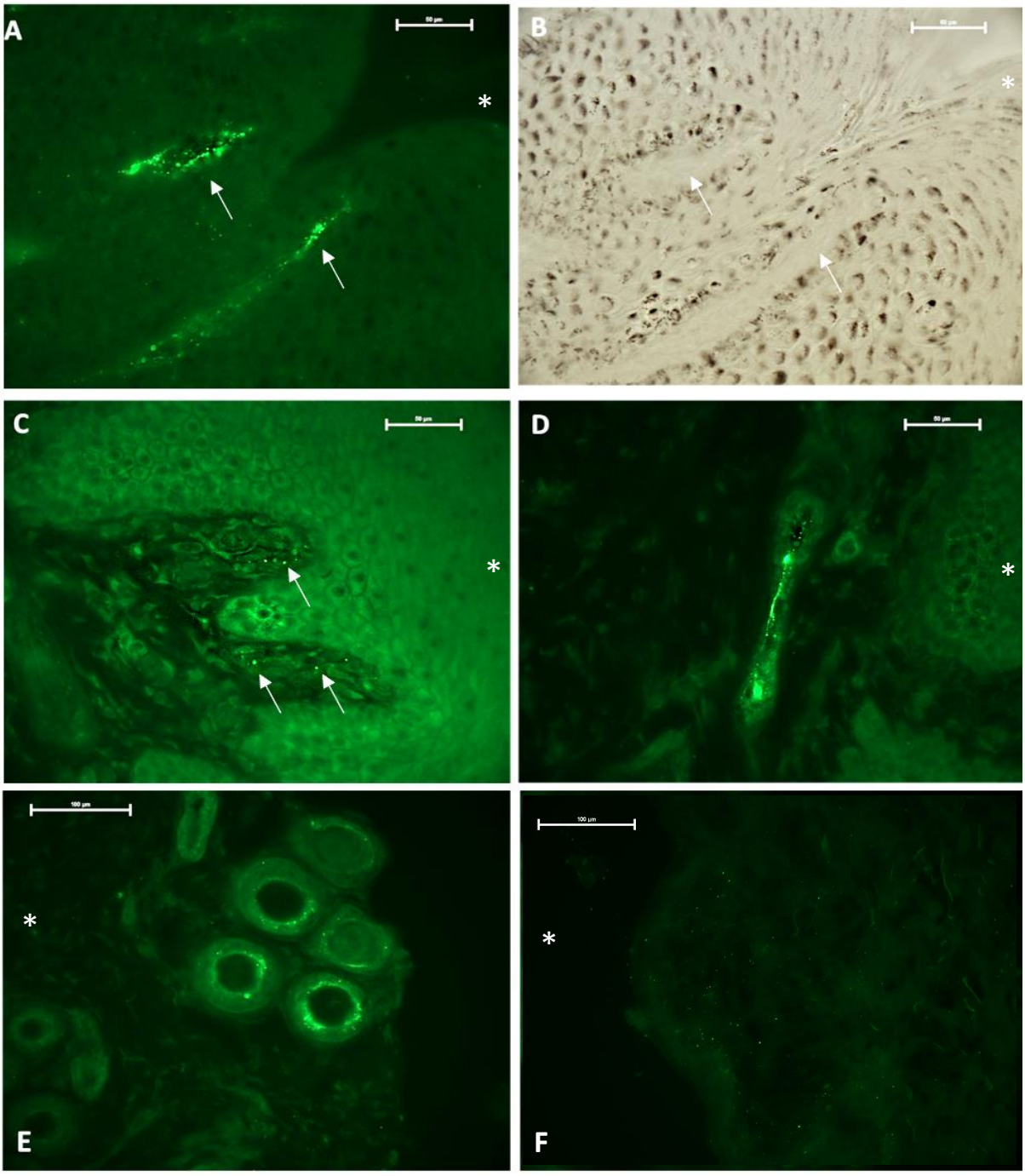

Figure 15: Immunohistochemical localisation of TRPV2 in mammalian skin. A: dog F rhinarium tissue, illustrating TRPV2 signal within the dermal papilla. B: B: Histological reference image to image A, indicating structural location of TRPV2 signal within the dog rhinarium tissue. C: bear rhinarium tissue showing TRPV2 signal in the dermal papilla. D: bear rhinarium tissue showing TRPV2 signal within an unknown structure. E: bear belly tissue showing TRPV2 signal within the hair follicles. F: dog F belly tissue showing no specific TRPV2 signal. White arrows indicate tissue location where TRPV2 signal is found. Asterisks indicates orientation of tissue section, indicating skin surface. Scale: 100 µm.

Localisation of TRPV3

The localisation of TRPV3 in specific tissue was observed in various mammalian tissue (Figure 16). TRPV3 signal was present at the tip of the epidermal pegs in the dog rhinarium tissue, within cells that are not known to illustrate auto-fluorescence (Figure 16: Image A). This is confirmed by the reference light microscopy image at the same location, indicating no structures that could auto-fluoresce (Figure 16: Image B). In both dog B and bears rhinarium tissue a diffuse TRPV3 signal was present throughout the dermis, with more specific signal in a nerve bundle and surrounding a blood vessel (Figure 16: Image C and D). The bear rhinarium tissue also had heavy TRPV3 staining of the keratinocytes (Figure 16: Image E). Lastly, dog M's belly and bear belly show TRPV3 signal in the hair follicles (Figure 16: Image E and F).

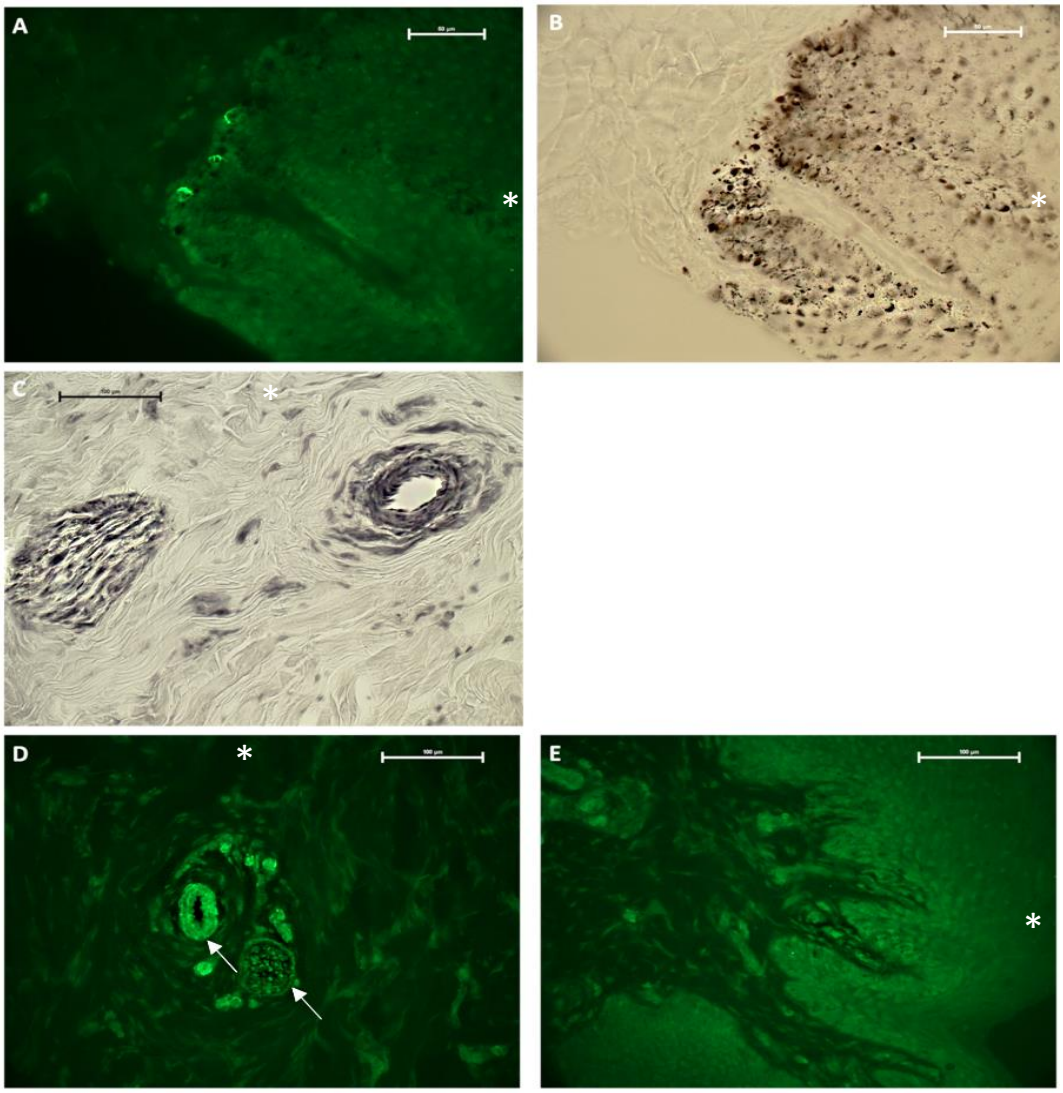

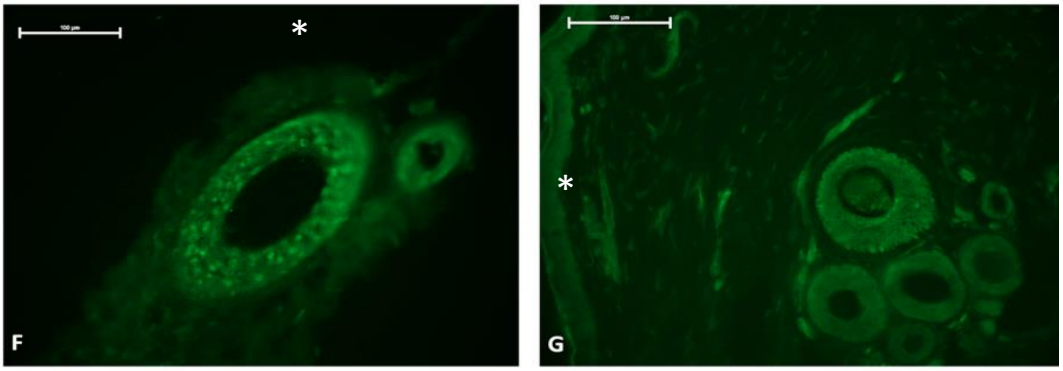

Figure 16: Immunohistochemical localisation of TRPV3 in mammalian skin: A: dog F rhinarium tissue showing TRPV3 signal at the tip of epidermal pegs. B: Histological picture of image A in same location showing what structures TRPV3 signal is within. C: dog B rhinarium tissue showing diffuse TRPV3 signal within the dermis and specific signal in the nerve bundle and blood vessels. D/E: bear rhinarium tissue showing diffuse TRPV3 signal in dermis and keratinocytes with specific signal in the blood vessels. F: dog F belly tissue showing specific TRPV3 signal with the hair follicles. G: bear belly tissue showing diffuse TRPV3 signal. White arrows indicate location of TRPV3 signal. Asterisks indicates orientation of tissue section, indicating skin surface. A/ B scale: 50 µm. C-G scale: 100 µm.

Localisation of TRPV4

The localisation of TRPV4 in specific tissues was observed in various mammalian tissue (Figure 17). TRPV4 signal was present at the tip of a dermal papilla protruding towards the surface of the dog F's rhinarium tissue, within cells that are not known to auto-fluoresce (Figure 17: Image A). Whereas, in the bear rhinarium tissue the TRPV4 signal was diffuse throughout the keratinocytes with more specific signal at the tip of the epidermal pegs and near the middle of a dermal papilla (Figure 17: Image C and D). Lastly, TRPV4 can be observed surrounding some blood vessels in the bear belly tissue (Figure 17: Image E).

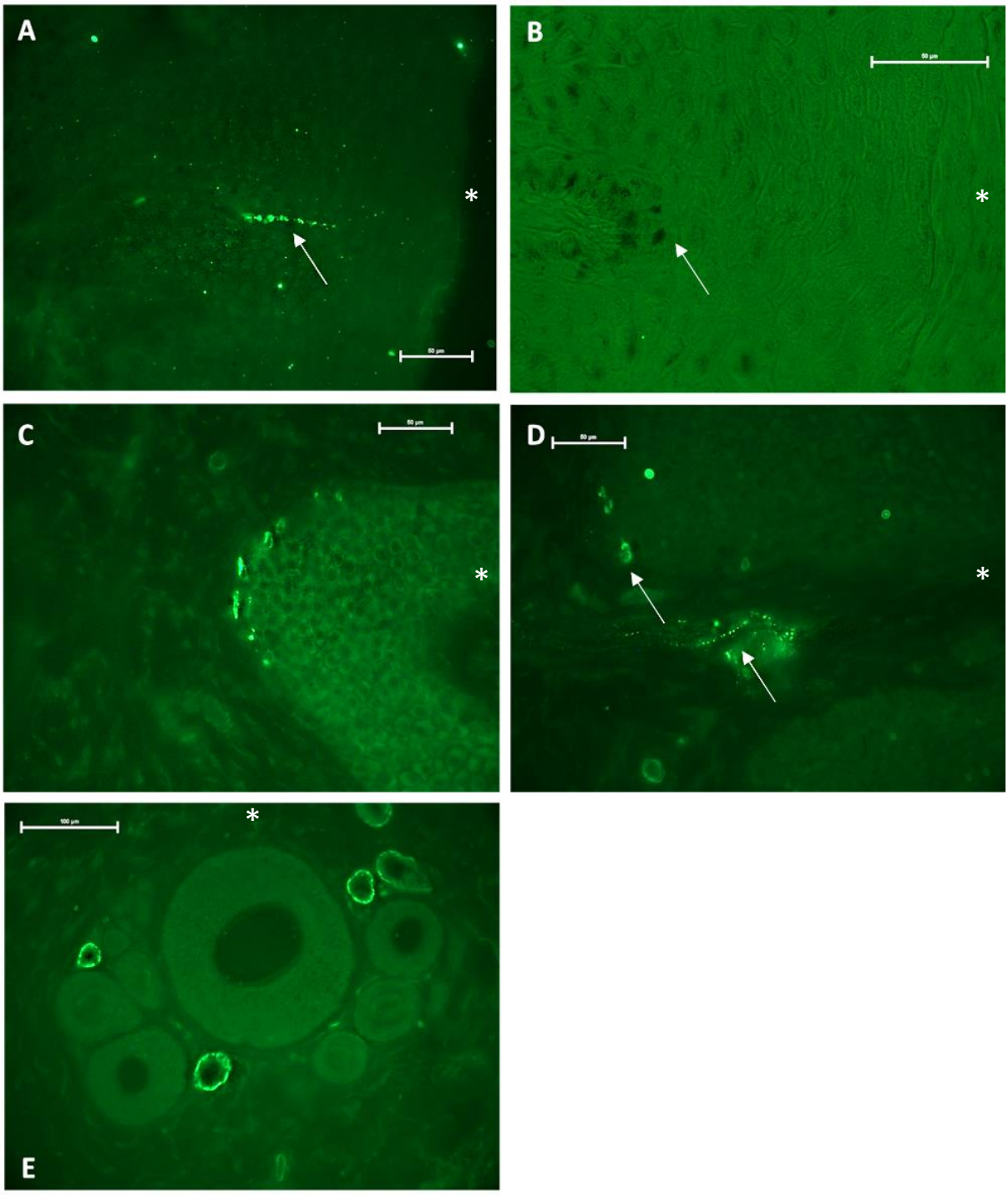

Figure 17: Immunohistochemical localisation of TRPV4 in mammalian skin: *A*: dog F rhinarium tissue showing TRPV4 signal coming from the tip of a dermal papilla. B: histological reference image to image A, illustrating its structural location within the tissue. C: bear rhinarium tissue showing TRPV4 signal at the tip of an epidermal peg. D: bear rhinarium tissue showing TRPV4 signal at the tip of an epidermal peg and at the bottom of a dermal papilla. E: bear belly tissue showing TRPV4 signal surrounding hair follicles. White arrows indicate TRPV4 signal. Asterisks indicates orientation of tissue section, indicating skin surface. A-D scale: 50 µm/ E scale: 100 µm.

Localisation of TRPM8

The localisation of TRPM8 in specific tissue was observed in various mammalian tissue (Figure 18) Within dog E's rhinarium tissue TRPM8 signal can be observed near the surface within the epidermis and in the dermis near the boundary to an epidermal papilla, within cells that are not known to auto-fluoresce (Figure 18: Image A, B and C). Lastly, TRPM8 is observed within the hair follicles of dog F and bear belly tissue (Figure 18: Image D and E respectively).

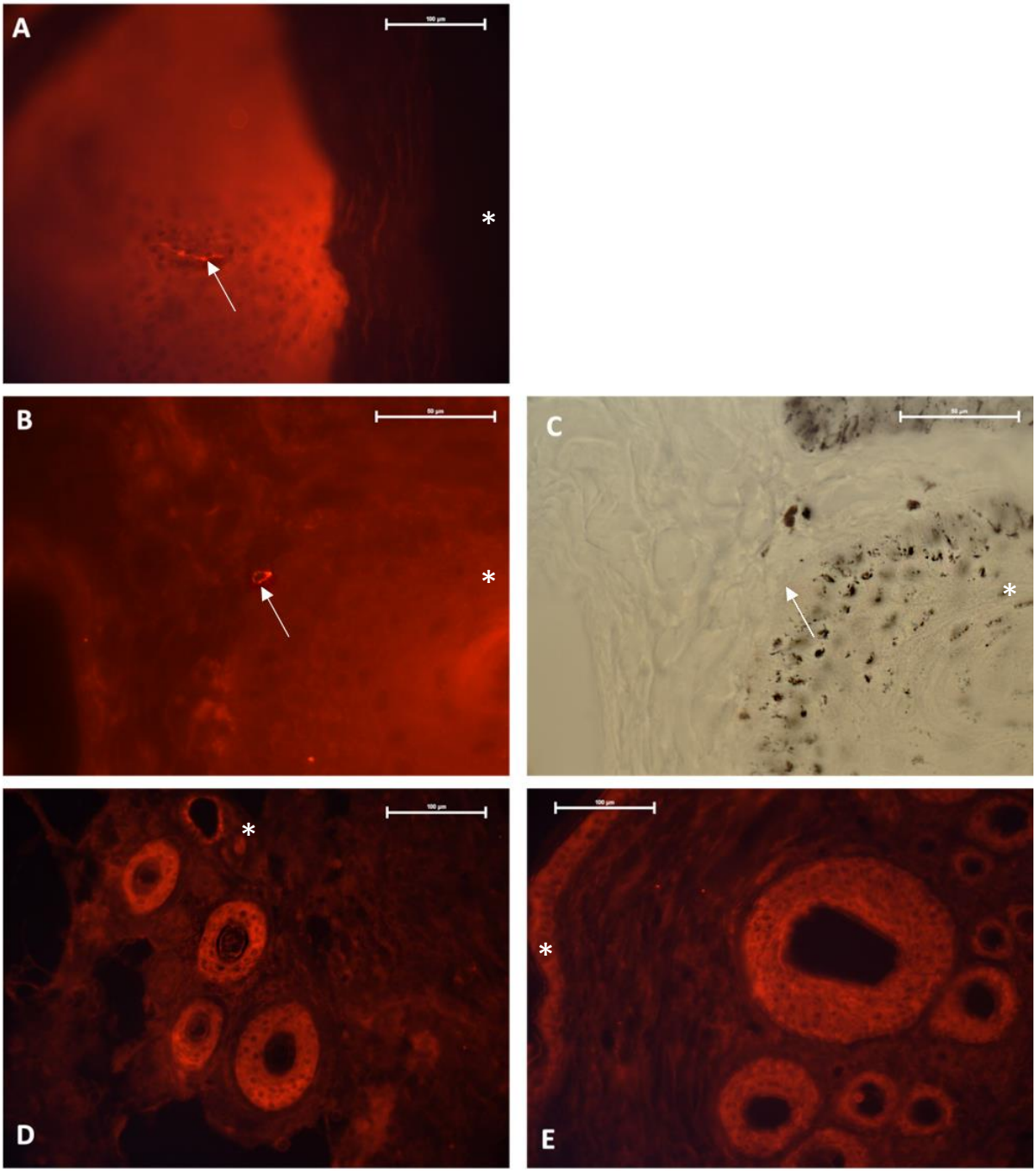

Figure 18: Immunohistochemical localisation of TRPM8 in mammalian skin. A/B: dog E rhinarium tissue showing TRPM8 signal within the epidermis and at the tip of an epidermal papilla respectively. C: Histological picture of image B in same location showing what structures TRPM8 signal is within. D/E: dog F and bear belly tissue respectively illustrating TRPM8 signal within the hair follicles. White arrows indicate TRPM8 signal. Asterisks indicates orientation of tissue section, indicating skin surface. A/D-E scale: 100 µm. B-C scale: 50 µm.

Mammalian Skin: Localisation of Nerve Network

The localisation of nerves were observed in various mammalian tissues (Figure 19). Within dog F's rhinarium tissue nerves can be seen within the epidermis reaching towards to skin surface and within the dermal papilla (Figure 19: Image A). A nerve bundle can be observed adjacent to a blood vessel in the dermis in dog F's rhinarium tissue (Figure 19: Image B). Within the bear rhinarium tissue nerves can be observed protruding from a dermal papilla and a nerve bundle can be observed within the dermis (Figure 19: Image E and F respectively). However, minimal nerve innervation can be observed in both the dog F and bear belly respectively (Figure 19: Image C and D respectively) by the green thread-like structures.

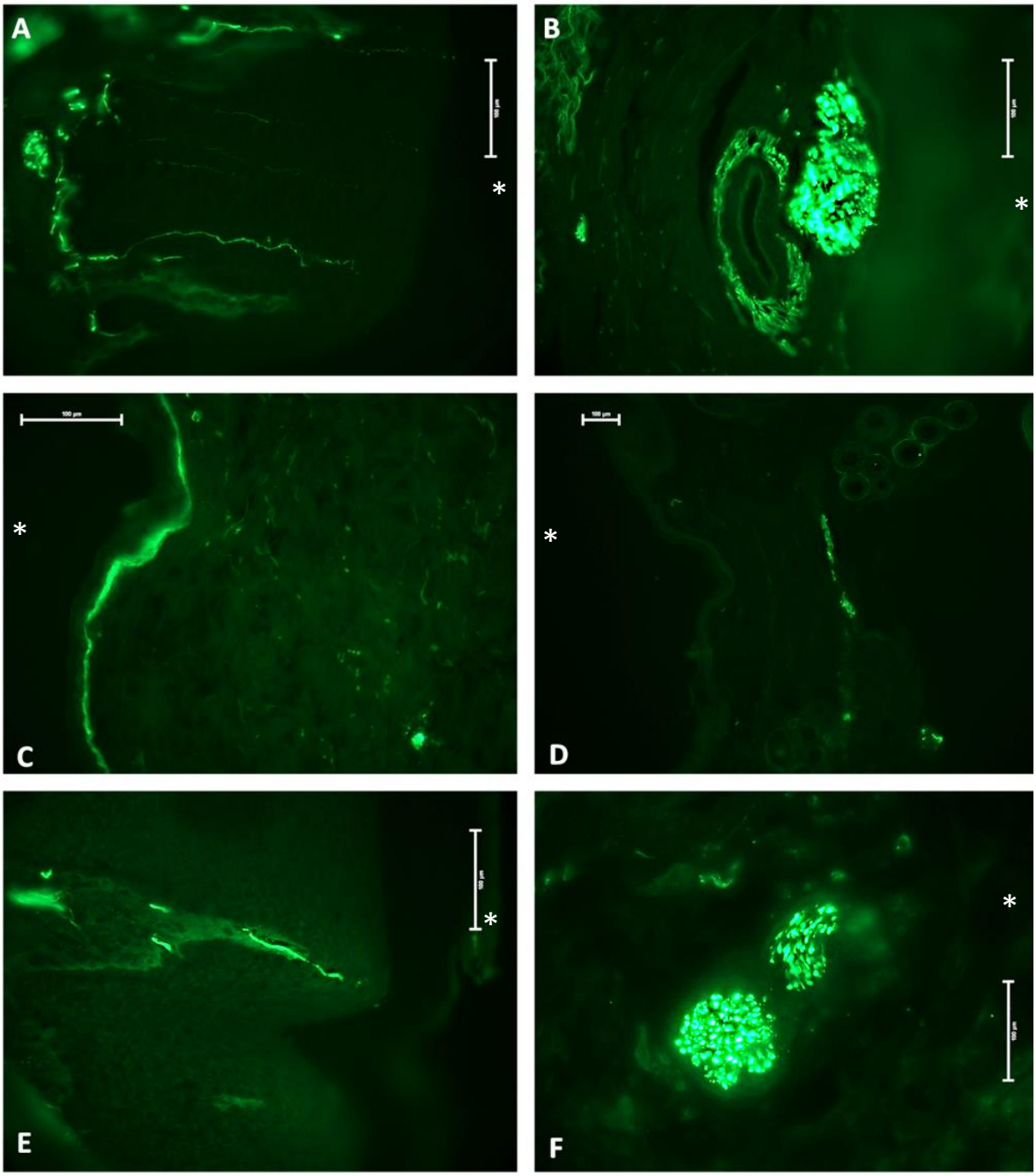

Figure 19: Immunohistochemical localisation of nerves fibers in mammalian skin. A: dog F rhinarium tissue illustrating nerve signal in the epidermis and within the dermal papilla. B: dog F rhinarium tissue illustrating a nerve bundle adjacent to a blood vessel in the dermis. C/D: dog F and bear belly tissue respectively illustrating minimal nerve innervation. E/F: bear rhinarium tissue sections showing nerves protruding from a dermal papilla and nerve bundles within the dermis respectively. Asterisks indicates orientation of tissue section, indicating skin surface. Scale: 100 µm

Table 4: Summary of results: *Summary of TRP channel localisation results in various mammalian skin types. [T] = tip of dermal papilla or epidermal peg, [B] – bottom of dermal papilla or epidermal peg*

Mammal	Skin type	TRPV1	TRPV2	TRPV3	TRPV4	TRPM8
Dog	Rhinarium	Dermal papilla [B] / epidermal pegs [T]	Dermal papilla [T]	Epidermal pegs [T]/ Epidermal keratinocytes/ Blood vessels/ Afferent nerve fibers	Signal protruding from dermal papilla [T]	Epidermal keratinocytes (unclear signal)/ dermal papilla [B]
	Paw	Removed from study due to auto-fluorescence				
	Belly	No indicated signal	No specific staining	Specific signal in Hair keratinocytes	No indicated signal	Hair keratinocytes
Lemur	Rhinarium	Removed from study due to auto-fluorescence				
	Paw					
	Belly					
Bear	Rhinarium	Epidermal peg [T]	Dermal papilla [T] (less than dog)/ dermis (unknown structure)	Epidermal keratinocytes/ Diffuse signal/ Blood vessels	Epidermal pegs [T]/ dermal papilla [B]	No indicated signal
	Paw	Removed from study due to auto-fluorescence				
	Belly	Diffuse signal	Hair follicles	Diffuse signal in hair keratinocytes	Hair follicles of certain size	Hair keratinocytes

Table 5: Basic Local Alignment Search Tool (BLAST) results: *BLAST results indicated that the primary antibodies used within these experiments have homology to the TRP channels of the Canis lupis familiaris indicating that they are conserved. Thus any fluorescent signal seen must be indicating the presence of a TRP channel.*

TRP channel primary antibody	Immunogen	Sequence	BLAST results (% identity to Canis lupus familiaris)
TRPV1 polyclonal antibody	A synthetic peptide corresponding to amino acids 608-621 human TRPV1.	PSESTSHRWRGPA	83%
TRPV2 polyclonal antibody	N-terminal domain of human.	RGKLDFGSGLPPMESQFQGEDRKFAPQI RVNLNYRKGTGASQPDPNRFDRDRLFNA VSRGVPEDLAGLPEYLSKTSKYLTDS	83%
TRPV3 polyclonal antibody	C- Terminal domain of rat	Whole TRPV3 sequence entered into Basic Local Alignment Search Tool (BLAST)	94%
TRPV4 polyclonal antibody	A synthetic peptide corresponding to 20 amino acid at internal region of human TRPV4	Whole TRPV4 sequence entered into Basic Local Alignment Search Tool (BLAST)	97%
TRPM8 polyclonal antibody	Synthetic peptide from the 1t cytoplasmic loop of Human TRPM8 conjugated to an immunogenic carrier protein.	Whole TRPM8 sequence entered into Basic Local Alignment Search Tool (BLAST)	96%

Discussion

The survival of mammals is reliant on sensing their environment, allowing them to respond appropriately. As discussed the skin is a sensory organ, containing a network of nerves which act as the link between the skin and the brain, enabling the animal to sense its environment. It is thought that temperature sensitive TRP channels are associated with these nerve ends and respond to changes in skin temperature.

The focus in this study was primarily the specialised rhinarium skin and its thermosensitive capabilities in both sensing radiating heat and protecting itself against thermal extremes. Furthermore, it was of interest to compare it to other mammalian tissue types. The observations discussed earlier were the motivations for this research.

We have hypothesised that a system must be in place that allows the rhinarium to protect itself against extreme thermal stimuli and allow sensitivity to radiating heat. Therefore, we assume the existence of superficial and deep TRP channel skin receptors to give a complete thermal picture. The receptors would cover the relevant temperature ranges as well as immediately warning against noxious temperatures. This system would act similarly to a bolometer (Schematic 1). In our hypothesised system the superficial TRP channel skin receptors, would sit near the skin surface. They would respond quickly to incoming thermal radiation and to conductive heat, causing a change in temperature. The superficial TRP channel skin receptors would therefore act as the absorptive element of the bolometer. The superficial TRP channel skin receptors would be thermally coupled via the tissue to the deep TRP channel skin receptors. The deep TRP channel skin receptors would sit lower in the skin and act as the thermal sink, monitoring the surrounding tissue temperature. A cold rhinarium would be required for this system to function as it would increase thermal sensitivity to small temperature changes by increasing the temperature differences between the two receptors. This system could also work for general thermosensitivity enabling quick response to noxious thermal stimuli. For this system TRPV1-4 and TRPM8 channels were of particular interest as at present there is strong evidence that they are involved in thermoreception in mammalian skin.

Promising results, which reflected our hypothesis, were seen in the rhinarium tissue. Unfortunately, all research on the paw tissue and lemur tissue had to be abandoned due to time constraints and problems caused by the innate auto-fluorescence of the tissue. All these results are discussed below.

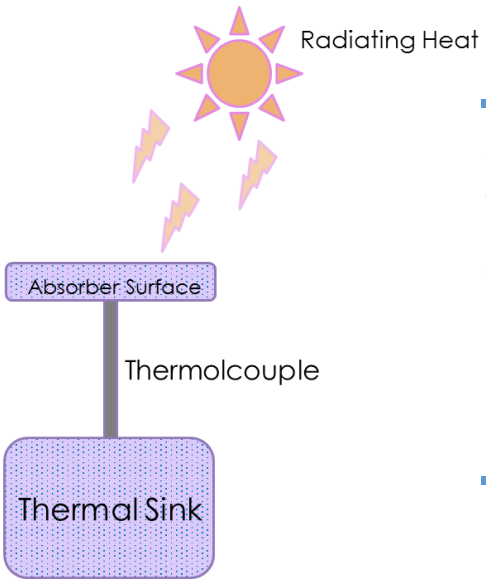

Schematic 1: Bolometer. *A bolometer described in its simplest form consists of an absorptive element and thermal sink which are thermally coupled to one another. Incoming radiation hits the absorptive element raising its temperature quickly above the thermal sink temperature, which is constant. A thermometer attached to the absorber element measures the change in temperature [2].*

Mammalian Skin: Auto-fluorescence

Natural and chemically induced auto-fluorescence within mammalian tissues can be a major issue when using florescence microscopy, causing false positives and shielding the true signal. Chemically induced auto-fluorescence can be caused by cross-links formed by the tissue fixative [18] or the compounds that are used within the experimental protocol. Naturally occurring auto-fluorescence is caused by specific cell types, such as keratinocytes.

During my study I encountered severe auto-fluorescence within all tissue samples, I recognised the auto-fluorescence by its appearance in both microscopy filter cubes. This caused the focus of the project to shift to try to correct this issue before returning to the original aims. The levels of auto-fluorescence can be observed in the auto-fluorescence control images (Figure 2-9). I focused on removing auto-fluorescence from the dog rhinarium skin sections as this tissue was of highest interest in the study.

The first approach was to remove Bovine serum albumin (BSA) from the method. It is known to have intrinsic florescence, naturally occurring fluorescence due to its two tryptophan residues[19]. Removing BSA from the protocol however did not reduce the auto-fluorescence (Figure 10: Image A and B). A chemical treatment was enlisted next, the tissue was subjected to an ethanol series (Figure 11: Image A). However, after the ethanol series the tissue still had a high level of auto-fluorescence. An acetone treatment (with citrate buffer) was also used. However, this treatment was not successful as a high level of auto-fluorescence could still be seen in the tissue (Figure 11: Image B). Photo-bleaching was also considered as it can potentially reduce auto-fluorescence[20], therefore, the previously ethanol and acetone treated tissue sections were subjected to strong light overnight. This method was also unsuccessful in removing the auto-fluorescence (Figure: 12: Image A and B). Lastly, a new immune-labelling method was tried using peroxidase anti-peroxidase (PAP) with 3, 3'-Diaminobenzidine (DAB) instead of fluorescence. The drawback of this method was the difficulties in distinguishing the signal in the heavily pigmented rhinarium tissue. A method to remove the pigment was performed but unfortunately this method failed to improve the results since the tissue was still heavily pigmented (Figure 13: Image A and B).

It was concluded that the auto-fluorescence could not be removed from these tissues. Therefore, new samples of frozen dog rhinarium tissue was tested. The tissue that was chosen had the shortest time between the death of the animal and fixation of the tissue. It was here I discovered that the auto-fluorescence in the previous tissues was caused by improper storage. The highly auto-fluorescent tissue had been stored in phosphate buffer in the refrigerator for several months. I arrived at this conclusion as the auto-fluorescence levels were drastically reduced within the frozen tissues. It is also evident that the level of auto-fluorescence has a positive correlation to the length of time between the death of the animal and the fixation of the tissue. It seems that the level of auto-fluorescence decreases with the decrease of time between death and fixation (Figure 2 and Table 1). The bear tissue samples illustrate virtually no auto-fluorescence, since the tissue was collected and fixated immediately after the animal's death, then prepared for sectioning the next day. This short time from collection to sectioning and further handling of the tissue insured the lowest level of auto-fluorescence. However, gathering rare tissue samples is problematic. The tissue samples have to be outsourced and are hard to come by, making storage an important factor to keep the integrity of the tissue in-tacked. To conclude, the tissue samples must be collected as soon as possible after the animal's death and if not used immediately they are stored at -80°C. The discovery of the importance of tissue storage will greatly improve future studies and allowed the original focus to be reinstated.

The problems with auto-fluorescence within the tissues should be kept in mind when observing the results below. The TRP channel expression signal seen is assumed to not be auto-fluorescence however this cannot be said for certain.

Mammalian Skin: Feeling the Heat

TRPV1's role in thermosensation

TRPV1, is known to respond to noxious heat, above 43°C which has been illustrated using knockout experiments in mice[11]. This channel has been found to be expressed in various locations, some of which have been seen in the experiments performed in this project. Figure 14: Image A suggests a TRPV1 signal located at the bottom of a dermal papilla and at the tip of an epidermal peg in dog rhinarium tissue. TRPV1 channels located here could act as deep TRP channel skin receptors, constantly monitoring the surrounding tissue temperature. TRPV1s expression has also been noted in this location within both thin human skin by Denda *et al* and B.Veronesi *et al* and in the dermal papilla of mouse frontal paws by J. Lakoma *et al* [21] *[22, 23]*. This indicates that the signal seen in Figure 14: Image A is most probably TRPV1 expression. However, focusing on the signal at the tip of the epidermal peg, it is of concern that this signal could be within a melanocyte (Figure 14: Image B), which are known to auto-fluoresce[24]. T. Choi *et al* have suggested that TRPV1 expression within these cells proposes their involvement in the signal transmission of cutaneous sensation, giving melanocytes a multifunctional role[25]. Our own confirmation that the expression is within structures that are not prone to auto-fluoresce comes from Figure 14: Image B. The signal pattern seen within the dog rhinarium tissue was also found within the bear rhinarium tissue, Figure 14: Image B, suggesting that the TRPV1 expression could be consistent across species.

Comparing the rhinarium tissue to the belly tissue, it would seem that there is a more diffuse TRPV1 signal within the belly tissue, it is not entirely clear why. However, the suggested TRPV1 signal within the hair follicles of the bear belly proposes that TRPV1 has a different function in this case (Figure 14: Image A). E. Bodó *et al* have implied that TRPV1 has a significant role in the hair growth cycle[26]. This could give reason for this signal pattern. Furthermore, TRPV1 is likely to have different functions within the belly skin due to its lack of exposure to surfaces. Heat sensation may not play an important role here.

As indicated in the literature TRPV1 is expressed within the C and Aδ-fibers, which terminate at the peripheral nerve endings in skin and respond to noxious and non-noxious cold[11, 15]. However, no TRPV1 expression was seen in the afferent nerve bundles of any tissue tested in our experiments. These heat sensitive nerve fibers would be crucial for the bolometer system as they are required for the fast transduction of the thermal signal. Therefore, it is unclear why there is no TRPV1 signal in the nerve bundles, indicating more experiments have to be performed.

TRPV2's role in thermosensation

TRPV2, like TRPV1 is also stimulated by noxious heat, however at higher temperatures above 52°C. TRPV2 has been found to be more widely expressed throughout the body[15], some of these locations have been demonstrated in my study. Figure 15: Image A illustrates TRPV2 signal extending towards the tip of two dermal papilla in dog rhinarium tissue. This could be interpreted as the superficial TRP channel skin receptor, responding to the initial elevation in temperature. H. E. Axelsson *et al* have also witnessed this pattern of TRPV2 expression within human skin[27]. Figure 15: Image B confirms that this signal is not within pigmented cells. Intriguingly, the bear rhinarium does not have an equally abundant TRPV2 signal as the dog rhinarium (Figure 15: Image C). This could indicate varied expression levels of TRPV2 between species, however further experiments have to be carried out. However, the TRPV2 signal in the same location, the dermal papilla, within the dog and bear rhinarium tissue (Figure 15: Image A and C), hints towards consistent expression across these species. In regards to the deep TRP channel skin receptors, TRPV2 signal is present just below the epidermal pegs in the dermis, however it is unclear what this structure is as a reference image is lacking. This structure has to be identified before further speculations can be made.

Within the bear belly the TRPV2 signal is localised to specific hair follicles. It is likely that the TRPV2 channels have an alternative function here. J. Lawson *et al* have proposed a mechanosensory function for TRPV2 after witnessing TRPV2 signal within low threshold mechanoreceptors (hair follicle afferents)[28]. Figure 15: Image E shows that the TRPV2 signal is within follicles of a specific size. However, this could be due to the level at which they were sectioned. Perhaps there is a higher abundance of TRPV2 channels responding to the mechanical stimuli closer to the follicle roots. Unlike

the bear belly, the dog belly showed no specific TRPV2 staining (Figure 15: Image F), this could indicate differences across these species but it is most probable that the tissue section was not at the appropriate level to visualise TRPV2 signal.

Similarly to TRPV1, TRPV2 is associated with Aδ-fibres, which transmit nociceptive information [15, 29]. Also like TRPV1 there was no TRPV2 signal seen within the afferent nerve bundles of the skin tested. It is unclear why this was the case and more research is therefore required.

TRPV3's role in thermosensation

TRPV3 unlike TRPV1-2 responds to non-noxious heat having a stimulus range of 34-38°C. TRPV3 has so far been seen to have a defined expression pattern throughout the body. Its association with nerve fibres has been under debate, which unfortunately was not any further resolved in my study.

Within the dog rhinarium the TRPV3 signal was of similar pattern and location as TRPV1's signal in dog and bear rhinarium. Figure 16: Image A illustrates TRPV3 signal at the tip of the epidermal pegs in dog F's rhinarium tissue. TRPV3 could act as the deep TRP channel skin receptors, monitoring the surrounding tissue temperature. W. Luo *et al* have produced similar results when using TRPV3 expression to identify Merkel cells within glabrous skin[30]. This type of cell are slow acting mechanoreceptors that are found at the base of epidermal pegs within ridged glabrous skin such as the rhinarium. They form mechanoreceptors with nerve terminals[30, 31]. Therefore, it is unclear if the TRPV3 channels expressed here are acting in thermal or mechanical transduction, indicating that more research is required to determine this. The bear rhinarium tissue did not exhibit the same signal pattern within the epidermal pegs as the dog rhinarium (Figure 16: Image A and E). TRPV3 expression within epidermal keratinocytes has been confirmed throughout literature [32-34]. We were able to illustrate this expression pattern in both the bear and dog rhinarium, Figure 16: Image E and A. Interestingly, M. Chung *et al* have hypothesised that this TRPV3 expression pattern in keratinocytes suggests that these cells may act in concert with sensory neurons. It was proposed that keratinocyte TRPV3 contributes to the perception of raised ambient temperatures via communication with sensory neurons by releasing diffusible messengers such as ATP or nitric oxide [11, 34, 35].

Intriguingly, both the bear and dog rhinarium show suggested TRPV3 signal associated with the blood vessels (Figure 16: C and D)). The literature suggests that TRPV3 has a role in vasodilation which would give reason for its expression here [36, 37]. Vasodilation is an excellent way to lose excessive heat therefore TRPV3 could have roles in maintaining the rhinarium at a cooler temperature[38]. This is necessary to increased thermal sensitivity for the bolometer system.

The ideas regarding TRPV3 expression within afferent nerve fibres remained conflicting after my study. Figures 16: Image C and D show TRPV3 signal in afferent nerve fibres within the dog rhinarium but not the bear rhinarium tissue respectively. H. Xu *et al* have also witnessed disparities between species TRPV3 expression within the sensory neurons, thus indicating inter-species variability[37]. However, J. Vriens *et al* and A. Peier *et al*, have hypothesised that the pattern of TRPV3 expression in the keratinocytes but not in sensory cells also indicates that TRPV3 mediates the sensation and discrimination of warm temperatures by the keratinocytes. As stated before keratinocytes may be communicating via chemical signalling. Unfortunately, animal models with disrupted or knocked out TRPV3 have so far been unable to reveal the full picture on their involvement in detection of heat [11, 14, 15].

TRPV3 expression is not only observed within epidermal keratinocytes but also hair follicle keratinocytes (Figure 16: Image F and G). We were able to reproduce these results within both the dog and bear belly tissue. Interestingly, the dog belly tissue seems to have more specific staining within hair follicles whereas the bear belly has a diffuse signal pattern (Figure 16: Image F and G). This could be due to inter-species differences. Interestingly, according to the literature, TRPV3 does not seem to have a mechanosensory function, which would be thought due to its expression within the hair follicles. However, J. Vriens *et al* and A. Peier *et al*, hypothesis of thermosensation via chemical signalling could also come into play in this situation [11, 35].

TRPV4's role in thermosensation

TRPV4 is within the same bracket as TRPV3, responding to non-noxious heat between 28-42°C. There is also some ambiguity over TRPV4 association with nerve fibres [11, 15-17]. However, like TRPV3 it is confirmed to be expressed in keratinocytes[11].

We were able to illustrate very specific staining of TRPV4 protruding from the tip of a dermal papilla into the epidermis in dog rhinarium (Figure 17: Image A). This pattern of staining could not be seen in the literature, however it is a good candidate for a superficial TRP channel skin receptors as they need to sit close to the skin surface if they are to be involved in detecting heat radiation and conductive heat transfer. Figure 16: Image B confirms this result and indicates that the signal does not sit within structures that are prone to auto-fluorescence. We were unable to find this signal pattern in any other tissue. The explanation for this may be that the channels sit at the very tip of the dermal papilla, therefore the probability of sectioning the tissue at the correct level, where the dermal papilla is at its longest, is very unlikely. In contrast, TRPV4 signal was observed at the tip of the epithelial pegs and at the bottom of dermal papilla, this was not seen within the dog rhinarium tissue (Figure 17: Image C and D). This pattern seen in the bear rhinarium but not dog rhinarium tissue could indicate inter-species differences. The expression pattern visualised in the bear rhinarium was similar to the TRPV1 and TRPV3 signal pattern. It is proposed that the structures expressing TRPV4 could be merkel cells, as they reside in this location and they are known to express TRPV4[39]. Therefore, I suggest that the TRPV4 channels here are acting as mechanoreceptors. Similar TRPV4 signal at the bottom of a dermal papilla has been observed in the bear rhinarium. If the hypothesis is to be correct the TRPV4 channels residing here act as deep TRP channel skin receptors, monitoring surrounding tissue temperature. However, M. Suzuki *et al* also found that TRPV4 is expressed in the Meissner's corpuscle cells[39]. These cells are known to sit in the dermal papilla[40], and like the Merkel cells, they respond to mechanical stimuli[39]. It seems probable that TRPV4's main function is mechanoreception.

Nevertheless, there is a complex network of free nerve endings within the dermis [41] and TRPV4 could be associated with these nerve endings allowing thermotransduction. However, due to the ambiguity over TRPV4 association with nerves, more research has to be carried out to determine the function of TRPV4 in mammalian skin.

Similarly to TRPV2 expression within the bear belly, TRPV4 also seemed to be expressed within hair follicles of a certain size (Figure 17: Image E). However, it is unclear if TRPV4 is expressed in non-specialised hair cells. According to the literature TRPV4 is expressed in auditory hair cells and functions as a mechanoreceptor [42, 43]. Its expression in non-specialised hair cells has not been determined yet. Expression within this location has to be confirmed first before TRPV4 function can be unravelled in regards to the bolometer hypothesis.

Mammalian Skin: Feeling the Cold

TRPM8's role in thermosensation

Sensing the cold is just as important as sensing heat. Many mammals reside in freezing climates, however it is unclear how these animals sense freezing temperatures and how they protect their glabrous skin from them. TRPM8 has been shown to function as a thermosensor in the skin with sensitivity to temperature ranges between<15-28°C. TRPM8 is expressed in various locations within the skin. We discovered some difficulty in localising the TRPM8 channels within the skin tissue used in this project. Potential TRPM8 expression was visualised but it is unclear if this was true signal as it was very weak. This signal was seen in dog rhinarium skin, within the keratinocytes of the epidermis (Figure 18: Image A). TRPM8 is known to be expressed within this location [44] therefore, this could be a candidate for a superficial receptor, which would respond rapidly to noxious cold. M. Denda *et al* demonstrated that keratinocytes were activated by low temperatures, whereas only a few nerve cells were activated[44]. They have hypothesised, like many others, that the epidermal keratinocytes have multiple thermo-sensitive systems covering a wide range of temperatures. TRPM8 in the epidermal keratinocytes might play a crucial role in skin cold thermosensation[44]. Suggested TRPM8 signal was also seen at the bottom of a dermal papilla in a structure not prone to auto-fluorescence (Figure 18: Image B and C). However, such an expression pattern has not been reported. Like the other TRP channels TRPM8's expression has been located to C and Aδ-fibres. Therefore, it could be suggested that within the dermal

papilla TRPM8 is associated with nerve endings[45]. Unfortunately, we were unable to localise TRPM8 within any of the other rhinarium tissues. The reason for this is unclear indicating more research is required to determine TRPM8 expression within other species.

In contrast TRPM8 expression was seen within both the bear and dog belly hair follicles (Figure 18: Image D and E). It is unclear what the function of TRPM8 is in this location as current literature does not support it. However, as stated before, it is expressed in epidermal keratinocytes. It is therefore likely that it is also expressed within hair keratinocytes.

Behavioural studies described in the literature have illustrated mice deficient in TRPM8 having a marked deficit in avoiding cool temperatures. In comparison wild type mice showed a strong preference to temperatures ~30°C over the cooler temperatures[11]. However, it has been suggested that TRPM8 is not the sole cold sensing channel and that there must exist a channel that detects exclusively noxious cold. TRPA1 is a prominent but controversial candidate for this role[11]. Potentially, it would be interesting to determine the location of this TRP channel within our tissue types and unravel its role in thermosensitivity.

Mammalian Skin: The Nerve Network

There is an extensive network of nerves within the skin. In the deeper portions of the dermis the nerves are thick, and closer to the epidermis the nerves become thinner[46]. These nerves, Aδ and C-fibres, are essential for conveying thermal information. As discussed previously, the TRP channels are believed to be associated with both these nerve types. Figure 19 (Image A, B, E and F) demonstrate the rich innervation of dog and bear rhinarium tissue. Many nerves terminate very close to the skin surface and protrude from the dermal pegs (Figure 19: Image A and E). With so much innervation near the surface of the skin it is unlikely that no temperature stimuli are being sensed here. Therefore the TRP channels expressed in these nerves could be acting as superficial TRP channel skin receptors. Indeed, some have been described with the free nerve endings in this study. The larger nerve bundles visualised in both the bear and dog rhinarium (Figure 19: Image B and F) could be home to the TRP channels functioning as the hypothesised deep TRP channel skin receptors. Lastly, we see innervation of the blood vessels within the dog rhinarium tissue (Figure 19: Image B). TRP channels are associating with the nerves here, it hints towards a role in blood temperature monitoring via vasodilation control.

In comparison to the rhinarium skin the belly tissue seems to be far less innervated (Figure 19: Image C and D). This could indicate less sensitivity in the belly tissue. One must keep in mind that the rhinarium skin is a highly specialised tissue. It is exposed to many more stimuli than the belly, and therefore should have more sensory cells as well as systems to defend itself against the surfaces it's exposed to.

Summary: Location of Superficial and Deep TRP Channel Skin Receptors

In relation to the hypothesis it would be reasonable to assume that temperature sensitive channels acting as superficial TRP channel skin receptors are associating with the mass network of free nerve endings close to the skin surface. The reasoning behind this is that the superficial TRP channel skin receptors will have to respond quickly to thermal stimuli at the tissue surface as it may be noxious. Therefore, by associating with the free nerve endings of Aδ and C fibres the stimulus signal can be transduced within milliseconds via action potentials. Another key element that is required for the bolometer system to work is deep TRP channel skin receptors. My results have shown an abundance of TRP channels associating with keratinocytes at the tip of epidermal pegs. The TRP channels here could be acting as deep TRP channel skin receptors. This is probable as keratinocytes are believed to be involved in thermoreception via chemical signalling, which is much slower than action potentials. This is in concordance with the hypothesis as the deep TRP channel skin receptors do not require fast transduction of the stimulus signal as they are continuously monitoring the surrounding tissue temperature, which remains somewhat constant.

Concluding Remarks

Through this study I wanted to understand how the rhinarium protects itself from thermal extremes and if the cooler temperature of the rhinarium might increase its sensitivity to sense radiating heat from the environment.
Our hypothesised biological bolometer-like system, which contained superficial and deep TRP channel skin receptor responding to thermal stimuli, has been somewhat supported by the results produced from my TRP channel localisation studies. All five TRP channels were visualised in locations that suggest deep TRP channel skin receptors. However, only 3 TRP channels, TRPV2, TRPV4 and TRPM8, were seen in locations that would be suited for the functioning of superficial TRP channel skin receptors. Furthermore, I was able to illustrate some discrepancies in TRP channel expression between mammalian species of different. However, this result is far from conclusive and requires more research. Furthermore, due the removal of the Lemur from the study no climate comparisons can be made.

The results from this study also illustrated how specialised and potentially sensitive to thermal stimuli the rhinarium tissue is compared to the belly skin. The rhinarium demonstrated itself to be a tissue with a vast network of nerves creating a highly sensitised tissue that can respond to many stimuli.

Lastly, through the loss of many tissue samples to auto-fluorescence in this study we now have a stronger grasp on how to reduce and/or prevent auto-fluorescence from occurring. Therefore, it must be maintained at a low level in future Immunohistochemical studies if one wishes to further understand how the thermally sensitive TRP channels are expressed in various mammalian tissue types.

Acknowledgments

I would like to express my gratitude to my supervisor, Prof. Ronald Kroger, for excellent guidance, support, and patience throughout my project. Furthermore, to my Co-supervisor, Prof. Rolf Elofsson who shared his extensive knowledge of skin with me and encouraged me throughout the writing process (Nulla dies sine linea). I would also like to thank Inga Tuminaite for also being a massive support throughout my whole research project and providing me with endless supplies of skin tissue. Lastly, I would like to thank Carina Rasmussen for her expertise in the laboratory and Sigrún Harpa Þórarinsdóttir for aiding me in image editing.

Works Cited

1. Vogelsang, E. *What the Fauna*. Tumblr 2015; Available from: http://whatthefauna.tumblr.com/post/99564767432/a-dogs-rhinarium-or-wet-nose-is-essential-for.
2. Nord, M., *Semiconducting Bolometers for Dummies.* 2006: p. 1-8.
3. Proksch, E., M. Brandner, and M. Jensen, *The skin: an indispensable barrier.* Experimental Dermatology 2008. **17**(12): p. 1063-1072.
4. Feingold, R., *The importance of lipids in cutaneous function.* Journal of Lipid Research 2007. **48**: p. 2529-2530.
5. Joseph, T., M. Daly, and R. Buffenstein, *Skin morphology and its role in thermoregulation in molerats, Heterocephalus glaber and Cryptomys hottentotus.* Journal of Anatomy 1998. **193**: p. 495–502.
6. Farage, M., A , et al., *Skin, Mucosa and Menopause: Management of Clinical Issues*. 1st ed. 2014: Springer.
7. Kröger, R. and N. Gläser, *Personal comunication* 2014.
8. Lahunta, A. and E. Howard, E, *Miller's Anatomy of the Dog*. 2013, Elsevier. p. 63-65.
9. Krause, W., J, *Krause's Essential Human Histology for Medical Students*. 2005: Universal-Publishers.
10. Pogorzala, L., S. Mishra, and M. Hoon, *The cellular code for mammalian thermosensation.* The Journal of Neuroscience 2013. **33**(13): p. 5533-5541.
11. Vriens, J., B. Nilius, and T. Voets, *Peripheral thermosensation in mammals.* Nature Reviews Neuroscience 2014. **15**: p. 573-589.
12. Tuminaite, I., *Masters Thesis: Are dog noses too cool for the mammalian cold receptor TRPM8.* 2015.
13. McAexander, M. and M. Moran, *Transient receptor potential channels as therapeutic targets.* Nature Reviews Drug Discovery, 2011. **10**: p. 601-620.
14. Tominaga, M. and M. Caterina, *Termosensation and Pain.* Journal of Neurobiology 2004. **61**(1): p. 3-12.
15. Wetsel, C., *Sensing hot and cold with TRP channels.* International Journal of Hyperthermia, 2011. **4**(27): p. 388-398.
16. Bíró, M. and T. Steinhoff, *A TR(I)P to Pruritus Research: Role of TRPV3 in Inflammation and Itch.* Journal of Investigative Dermatology 2009. **129**(3): p. 531-535.
17. Smith, G., D , M. Gunthorpe, J, and R. Kelsell, E, *TRPV3 is a temperature-sensitive vanilloid receptor-like protein.* Nature, 2002. **418**: p. 186-190.
18. Wright-Cell-Imaging-Facility, *Autofluorescence: Causes and Cures*. 2015: Toronto Western Research Institute University Health Network.
19. Silva, D., M. Cortez, and W. Louro, *Quenching of the intrinsic fluorescence of bovine serum albumin by chlorpromazine and hemin.* Brazilian Journal of Medical and Biological Research, 2004. **37**: p. 963-968.
20. Gabel, M. and D. Neumann, *Simple Method for Reduction of Autofluorescence in Fluorescence Microscopy.* The Journal of Histochemistry & Cytochemistry, 2002. **50**(3): p. 437-439.
21. Denda, M., S. Fuziwara, and K. Inoue, *Immunoreactivity of VR1 on epidermal keratinocyte of human skin.* Biochem Biophy Res Commun 2001. **285**(5): p. 1250-1252.
22. Oortgiesen, B. and M. Veronesi, *The TRPV1 Receptor: Target of Toxicants and Therapeutics.* Toxicological Science, 2005. **89**(1): p. 1-3.
23. Lakoma, J. and R. Rimondini, *Pain related channels are differentially expressed in neuronal and non-neuronal cells of glabrous skin of fabry knockout male mice.* PLOS ONE, 2014. **9**(10): p. 1-12.
24. Sandby-Møller, J., T. Poulsen, and H. Wulf, *Influence of epidermal thickness, pigmentation and redness on skin autofluorescence.* Photochemistry and Photobiology, 2003. **77**(6): p. 616-620.

25. Choia, T., S. Parkb, and J. Jo, *Endogenous expression of TRPV1 channel in cultured human melanocytes.* Journal of Dermatological Science, 2009. **56**(2): p. 128-130.
26. Bodó, E., T. Bíró, and A. Telek, *A hot new twist to hair biology: involvement of vanilloid receptor-1 (VR1/TRPV1) signaling in human hair growth control.* American Journal of Pathology, 2005. **166**(4): p. 985-98.
27. Axelsson, H., E and J. Minde, K, *Transient receptor potential vanilloid 1, vanilloid 2 and melastatin 8 immunoreactive nerve fibers in human skin from individuals with and without norrbottniam congenital insensitivity to pain.* Neuroscience, 2009. **162**(4): p. 1322-1332.
28. Lawson, J. and S. Mcllwrath, *TRPV1 Unlike TRPV2 is Restricted to a Subset of Mechanically Insensitive Cutaneous Nociceptors Responding to HeatJ.* The Journal of Pain, 2008. **9**(4): p. 298-308.
29. Jiang, K. and N. Rau, *Heat sensitization in skin and muscle nociceptor expressing distinct combinations of TRPV1 and TRPV2 protein.* Journal of Neurophysiology, 2007. **97**(4): p. 2651-2662.
30. Luo, W., H. Enomoto, and F. Rice, *Molecular Identification of Rapidly Adapting Mechanoreceptors and Their Developmental Dependence on Ret Signaling.* Neuron, 2009. **64**: p. 841-856.
31. Halata, Z., M. Grim, and K. Bauman, I, *Friedrich Sigmund Merkel and His "Merkel Cell", Morphology, Development, and Physiology: Review and New Results.* The anatomical record. Part A, Discoveries in molecular, cellular, and evolutionary biology, 2003. **271**(1): p. 225-239.
32. Misery, N. and L. Boulais, *The epidermis: a sensory tissue.* Eur J Dermatol, 2008. **18**(2): p. 119-127.
33. Luo, J., et al., *Tonic Inhibition of TRPV3 by Mg2+ in Mouse Epidermal Keratinocytes.* Journal of Investigative Dermatology, 2012. **132**(9): p. 2158-2165.
34. Chung, M., H. Lee, and A. Mizuno, *TRPV3 and TRPV4 Mediate Warmth-evoked Currents in Primary Mouse Keratinocytes.* The Journal of Biological Chemistry 2004. **279**(20): p. 21569-21575.
35. Peier, A., A. Reeve, and D. Andersson, *A Heat-Sensitive TRP Channel Expressed in Keratinocytes.* Science, 2002. **296**: p. 2046-2049.
36. Earley, S., A. Gonzales, L, and Z. Garcia, I, *A Dietary Agonist of Transient Receptor Potential Cation Channel V3 Elicits Endothelium-Dependent Vasodilation.* Molecular Pharmacology, 2010. **77**(4): p. 612-620.
37. Xu, H. and I. Ramsey, S, *TRPV3 is a calcium-permeable temperature-sensitive cation channel.* Nature, 2002. **418**: p. 181-185.
38. Charkoudian, N., *Mechanisms and modifiers of reflex induced cutaneous vasodilation and vasoconstriction in humans.* Journal of Applied Physiology 1985. **109**(4): p. 1221-1228.
39. Suzukia, M. and Y. Watanabe, *Localization of mechanosensitive channel TRPV4 in mouse skin.* Neuroscience Letters, 2003. **353**: p. 189-192.
40. Klauer, G., H. Burda, and E. Nevo, *Adaptive Differentiation of the Skin of the Head in a Subterranean Rodent, Spalax ehrenbergi.* Journal of Morphology, 1997. **233**: p. 53-66.
41. Tschachler, M., E and C. Reinisch, *Sheet Preparations Expose the Dermal Nerve Plexus of Human Skin and Render the Dermal Nerve End Organ Accessible to Extensive Analysis.* Journal of Investigative Dermatology, 2004. **122**: p. 177-182.
42. Liedtke, W. and Y. Choe, *Vanilloid receptor-related osmotically activated channel (VROAC), a cadidate vertebrate osmoreceptor.* Cell 2000. **103**(3): p. 525-535.
43. Cuajungco, M., P, C. Grimm, and S. Heller, *TRP Channels as Cadidates for Hearing and Balance Abnormalities in vertebrates.* Biochemica et Biophysica Acta, 2007. **1772**(8): p. 1022-1027.
44. Denda, M., M. Tsutsumi, and S. Denda, *Topical application of TRPM8 agonists accelerates skinpermeability barrier recovery and reduces epidermalproliferation induced by barrier insult: role of cold-sensitive TRP receptors in epidermal permeability barrier homoeostasis.* The Journal of Experimental Dermatology, 2010. **19**(9): p. 791-795.

45. Dhaka, A., et al., *Visualizing Cold Spots: TRPM8-Expressing Sensory Neurons and Their Projections.* The Journal of Neuroscience, 2008. **28**(3): p. 566-575.
46. Elofsson, R., I. Tuminaite, and R. Kroger, *A Complex Sensory Organ in the Nose Skin of the Prosimian Primate Lemur catta.* Journal of Morphology 2015. **276**(6): p. 649–656.